



### 저작자표시-비영리-변경금지 2.0 대한민국

이용자는 아래의 조건을 따르는 경우에 한하여 자유롭게

- 이 저작물을 복제, 배포, 전송, 전시, 공연 및 방송할 수 있습니다.

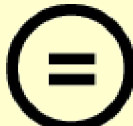
다음과 같은 조건을 따라야 합니다:



저작자표시. 귀하는 원 저작자를 표시하여야 합니다.



비영리. 귀하는 이 저작물을 영리 목적으로 이용할 수 없습니다.



변경금지. 귀하는 이 저작물을 개작, 변형 또는 가공할 수 없습니다.

- 귀하는, 이 저작물의 재이용이나 배포의 경우, 이 저작물에 적용된 이용허락조건을 명확하게 나타내어야 합니다.
- 저작권자로부터 별도의 허가를 받으면 이러한 조건들은 적용되지 않습니다.

저작권법에 따른 이용자의 권리와 책임은 위의 내용에 의하여 영향을 받지 않습니다.

이것은 [이용허락규약\(Legal Code\)](#)을 이해하기 쉽게 요약한 것입니다.

[Disclaimer](#)



# Microfluidic Concentrator Array for Quantitative Predation Study of Predatory Microbes



Seongyong Park

Thermofluid and Energy Systems Major  
School of Mechanical and Advanced Materials Engineering  
Graduate School of UNIST

2012

# Microfluidic Concentrator Array for Quantitative Predation Study of Predatory Microbes

A thesis

submitted to the School of Mechanical and Advanced Materials Engineering  
and the Graduate School of UNIST

in partial fulfillment of the  
requirements for the degree of  
Master of Science

Seongyong Park

01.17.2012

Approved by

---

Major Advisor  
Taesung Kim

# Microfluidic Concentrator Array for Quantitative Predation Study of Predatory Microbes

Seongyong Park

This certifies that the thesis of Seongyong Park is approved.

01.17.2012

---

Thesis Supervisor: Taesung Kim

---

Robert.J.Mitchell: Thesis Committee Member #1

---

Sungkuk Lee: Thesis Committee Member #2

## **Abstract**

Despite future impact on the bio-nano-technological application, the study of predatory microbes has been limited due to the complexity associated with co-cultures of prey and predator. In this thesis, to accelerate and simplify the study, we have developed a microfabricated concentrator array device that makes it possible to quantify the predation rate of predator, *Bdellovibrio bacteriovorus*. Since the concentrator array device can constrain both prey and predator cells within 200 pL chambers at a desired range of cell densities, the predation rates could be quantified indirectly by measuring the time-dependent fluorescent intensity signals from the prey. In addition, we study many different conditions with a single set of cultures because the device can produce a wide range of initial prey to predator density ratios within various concentrator arrays through the use of microfluidic gradient generator structures. We also investigated chemotaxis of *B.bacteriovorus* strain HD 100 using novel microfluidic concentration gradient generator towards various compounds and prey cell itself. The results were consistent with literatures.

## Contents

I . Introduction-----	1
1.1 Objectives -----	1
1.2 Microfluidic Concentrator Array Device -----	2
1.3 Microfluidic Chemotaxis Device -----	4
II . Quantitative Predation assay -----	6
2.1 Experimental Setup and Methods -----	6
2.1.1 Preparation of the prey, E. coli str. MG1655 -----	6
2.1.2 Bdellovibrio bacteriovorus culturing techniques -----	6
2.1.3 Microfluidic Concentrator Arrays for Motile Bacterial Cells -----	7
2.1.4. Fabrication of the microfluidic devices -----	7
2.1.5 Experimental procedure and data analysis -----	9
2.2 Results and Discussion -----	11
2.2.1 Experimental Configurations for the Concentrator Array -----	11
2.2.2 Concentration of motile microbes -----	11
2.2.3 Predation of prey (E. coli) at a single cell level -----	15
2.2.4 Predation of prey by predator at a multi-cell level -----	17
2.2.4.1 Uniform density of prey and uniform density of predator ( $UP_1 UP_2$ ) -----	17
2.2.4.2 Uniform density of prey and compartmentalization of predator ( $UP_1 CP_2$ ) -----	21
2.2.4.3 Uniform density of prey and linear density gradient of predator ( $UP_1 LP_2$ ) and linear density gradient of prey and uniform density of predator ( $LP_1 UP_2$ ) -----	22
2.2.5 Further applications of the device -----	26
III. Chemotaxis assay -----	27
3.1 Experimental Setup and Methods -----	30
3.1.1 Bacterial strains, materials, and growth media -----	30
3.1.2 Fabrication of microfluidic device -----	30
3.1.3 Construction of hydrogel plugs in micro channel -----	30
3.1.4 Quantification of chemotaxis using image analysis -----	31
3.1.5 Theoretical Analyses -----	31
3.2 Results and Discussion -----	33
3.2.1 Chemotaxis towards Yeast extract-----	33

3.2.2 Chemotaxis towards KCl-----	35
3.2.3 Chemotaxis towards D-glucose -----	38
IV. Conclusions -----	40
V . References -----	41

## List of figures

- Figure 1.1 The life cycle of *Bdellovibrio bacteriovorus*.
- Figure 1.2 Schematic of concentration gradient generator and experimental measurements of cell density gradients.
- Figure 1.3 Microfluidic concentration gradient generators.
- Figure 2.1 Microfluidic concentrator array device.
- Figure 2.2 Various experimental configurations.
- Figure 2.3 Concentration of predator and prey cells using the 10 by 3 concentrator array.
- Figure 2.4 Concentration of predator cells.
- Figure 2.5 Calibration curve for the calculation of the number of cells in the chamber.
- Figure 2.6 The observation of the predation at a single cell level.
- Figure 2.7 Fluorescence image of control and UP<sub>1</sub>UP<sub>2</sub> experiments.
- Figure 2.8 Compartmentalized predation and control experiments.
- Figure 2.9 Quantitative analysis of predation and control experiments.
- Figure 2.10 Results of UP<sub>1</sub>LP<sub>2</sub> experiments.
- Figure 2.11. Results of LP<sub>1</sub>UP<sub>2</sub> experiments.
- Figure 2.12 Quantitative results of UP<sub>1</sub>LP<sub>2</sub> and LP<sub>1</sub>UP<sub>2</sub> experiments.
- Figure 3.1 Diffusion based microfluidic concentration gradient generator ( $\mu$ CG).
- Figure 3.2 The procedure of image analysis of the number of *Bdellovibrio* cells.
- Figure 3.3 Chemotaxis of *B. bacteriovorus* toward various concentration of yeast extract.
- Figure 3.4 Quantitative data for the Chemotaxis assay of *B. bacteriovorus* towards various concentrations of KCl and D-glucose.
- Figure 3.5 Qualitative data for the Chemotaxis assay of *B. bacteriovorus* towards various concentrations of KCl and D-glucose.
- Figure 3.6 Representative figures for each experiment.

# Chapter I

## Introduction

### 1.1 Objective

Predatory prokaryotes, Bdellovibrio-and-Like-Organisms (BALOs), are unusual, small and highly motile gram-negative bacteria that invade the periplasm of other gram-negative bacteria and digest the cellular components within the prey cytoplasm<sup>1,2</sup>, as shown in Fig.1. 1. This unusual characteristic of BALOs has been the focus of many biologists and ecologists who desire to reveal the exact role of these predators in nature.<sup>3,4</sup> To date, the study of the predator is both a scientific curiosity and an essential step for the future application of bacterial predators to a variety of industrial fields, such as the development of alternatives therapeutic agents and in biofilm mitigation.<sup>5</sup> Although BALOs have been highlighted as one of the most applicable candidates within these fields, the study of BALOs has been limited due to the complexity associated with co-cultures of prey and predator as well as its fast motility, small size, and gene resistance. Objective of this thesis is measuring response of *B.bacteriovorus* on a microfluidic chip in various stimuli. At first, to quantify the predation rate by measuring green fluorescence protein (GFP) of the prey, we investigated single prey predation on our microfluidic chip.

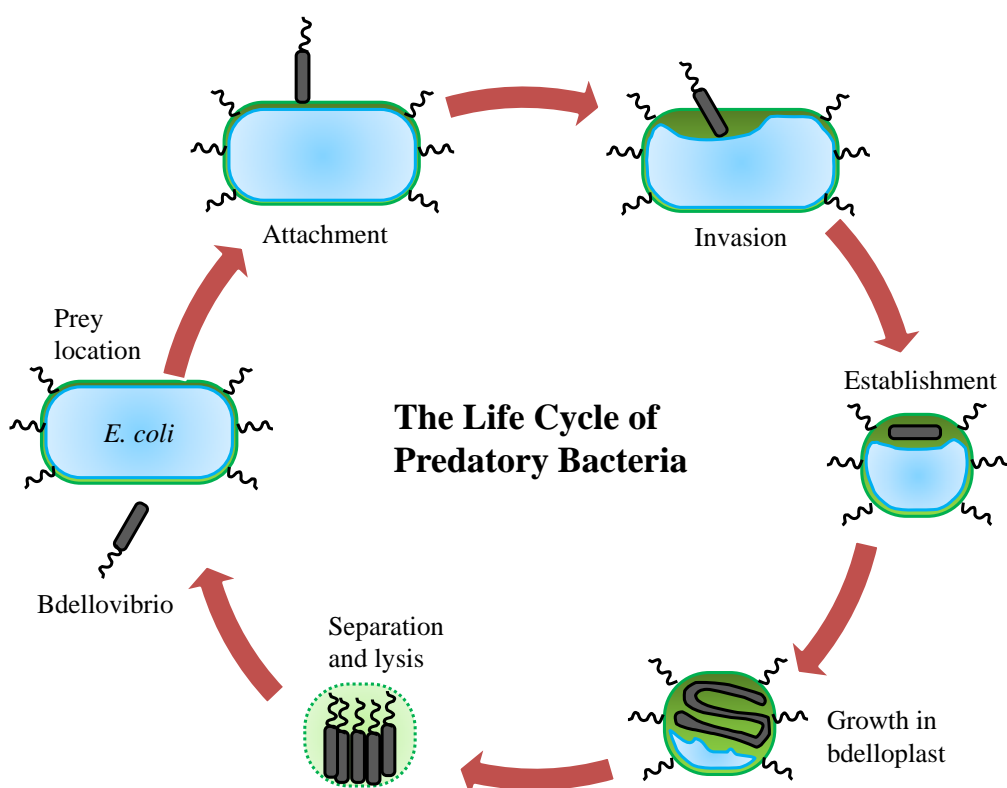


Fig 1.1 The life cycle of *Bdellovibrio bacteriovorus* in common prey, *Esherichia coli*.

When *B.bacteriovorus* free swimming phase meet the prey, it attaches the surface membrane of the prey to penetrate into the periplasm. After invasion, it consumes cytoplasm of the cell and finally lysis the cell to become progenitor cells.

In addition, we explored predation behaviour by utilizing Christmas tree shaped micromixer and microscopic ratchet structure in different predator to pray ratio conditions on a chip. Finally, we studied chemotactic responses of *B.bacteriovorus* towards various compounds and cells with a novel microfluidic concentration gradient generator. This introduction briefly describes the underlying principles of each microfluidic components. The organization of this thesis will be followed.

## 1.2 Microfluidic Concentrator Array Device

To investigate predation process, prey and predator cells should be constraint within the same chamber. Conventionally, this is achieved by culturing cells in the test tube or 96 well microplate which are too large compared to the size of prey and predator cells. To address the problem of conventional culture methods, we designed and fabricated new concept of device called microfluidic concentrator array device. Owing to the size of microfluidic devices,<sup>6,7</sup> which is typically a few micrometers in length, the device can offer an unprecedented means by which we can study the interaction between the predator and its prey.<sup>8,9</sup>

The device is composed of two main microfluidic components, such as Christmas tree shaped concentration gradient generator and concentrator unit. The gradient generator has been widely used to produce various concentration gradients in microfluidic devices.<sup>10,11</sup> These methods for generating a concentration gradient are well established and have also been used for studying the chemotactic behaviour of bacterial and mammalian cells.<sup>11,12</sup> In this thesis, however, we apply this concentration gradient generation mechanism to producing a density gradient of cells and to concentrating the microbes within the concentrator array using uniform or linear density gradients.

Another microfluidic component is concentrator unit. We utilized a microfabricated ratchet structure array for concentrating the motile microbes at a desired destination and the range of necessary densities.<sup>13,14</sup> Since motile microbes hold an intrinsic tendency to swim either on the right or left side in straight microchannels,<sup>15</sup> they can be guided to move along the microchannels and then trapped in certain chambers that incorporate arrowhead-shaped ratchet structures which prevent them from exiting. Several similar microfabricated mechanical patterns have been previously used to control the direction of bacterial cells<sup>16-18</sup> and biomolecular motors.<sup>19,20</sup>

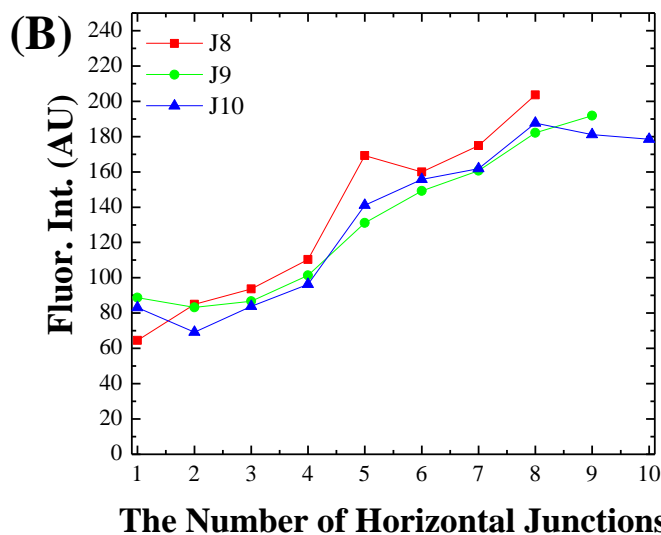
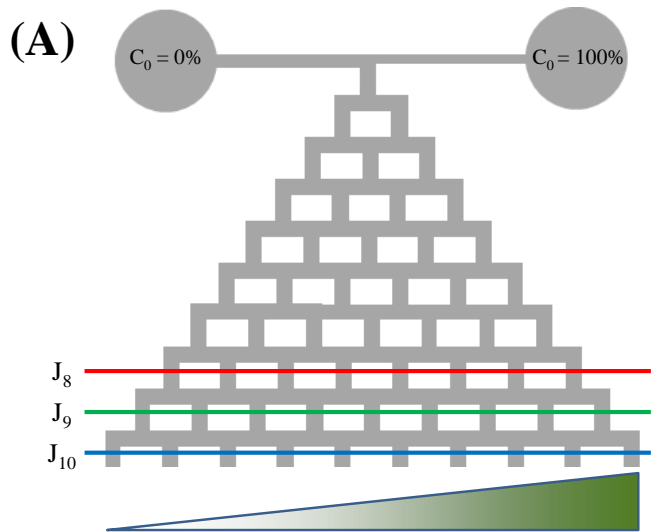


Fig 1.2 Schematic of concentration gradient generator and experimental measurements of cell density gradients. (A) Schematic of concentration gradient generator. When we load culture medium on left hand side and cell suspending medium on right hand side of reservoirs, it generate cell concentration gradient along the junctions. (B) Experimental results show that the concentration gradient of cells successively generated by this method and the gradient is  $k=1.4$ .

### 1.3 Microfluidic Concentrator Gradient Generator

Recent achievement on the bacterial chemotaxis research based on the microfluidics technology showed well how the microfluidic approach can help to understand more about the phenomena in quantitative manner<sup>21-23</sup>. Although conventional methods such as, Boyden chamber<sup>24</sup>, plate<sup>25</sup>, and capillary<sup>26</sup> chemotaxis assay offered chemical gradients to study chemotaxis, the gradients made by these methods are temporal and unstable which are not proper to the quantitative assay. Since microfabrication technology provides the ability to control micro environments by constructing microstructures on a substrate and microfluidics regulates fluid behavior in micro scale<sup>27</sup>, these technologies promise accurate and stable gradients compared to conventional methods. There are several advantages for the use of microfluidic gradient generator. First, channel geometries and chemical gradients can be controlled in  $\mu\text{m}$  resolution which is hard to achieve with conventional method. Second, because of the characteristic in the low Reynolds number flow, chemical gradients are smooth and mathematically predictable. Third, the platform is suitable for microscopy since the microfluidic chip is usually made by transparent materials, such as PDMS. Therefore, tracking of the individual cells in the chamber is possible<sup>21</sup>.

There are mainly two types of microfluidic chemotaxis testing devices. One is flow based gradient generator and another is diffusion based gradient generator. Flow based device is advantageous in gradient generating time but the device continuously applying shear force to the target cells.<sup>22</sup> Owing to the high motility of *Bdellovibrio*, instead of flow based device, we employed diffusion based device although gradient generation time in diffusion based or flow free device takes longer than flow based device.<sup>28</sup> To perform chemotaxis assay for predatory bacteria, we utilizes previously developed hydrogel plugging method used to construct chemical gradients in a microfluidic device.<sup>12</sup>

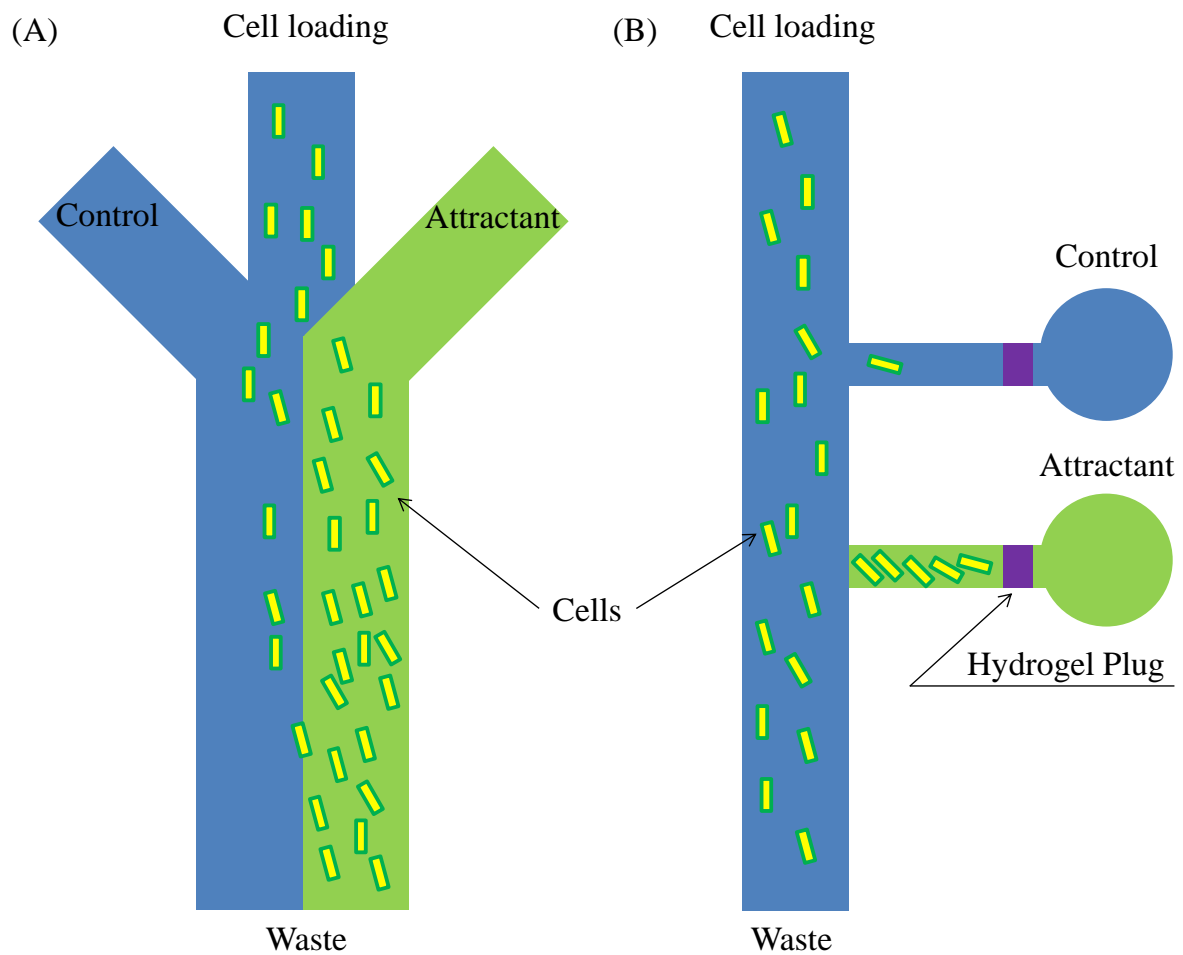


Fig 1.3 Microfluidic concentration gradient generators. (A) A typical Y shaped flow based concentration gradient generator. Since the nature of flow in micron scale, i.e. laminar flow, attractant diffuse control medium predictably and attract cells. (B) Hydrogel plug diffusion based microfluidic concentration gradient generator shear stress on the target cells.

## Chapter II

### Quantitative predation assay

In this work, we present a novel microfluidic concentrator array device that can both characterize predation rates at a variety of cell densities and analyse the predatory behaviour of BALOs at a single cell level under various experimental conditions. First, we demonstrate that concentric circular channels connected with arrowhead-shaped ratchet structures concentrate both the predator and prey microbes in the array with a uniform, square wave and linear density gradient along the array. Second, we demonstrate that the array device can be used to quantify the fluorescent signals from prey cells that express a fluorescent reporter gene during the predation process and that it is possible to employ these values to study the overall predation rates. Third, we demonstrate the versatile abilities of this device to provide varied experimental configurations associated with the types of prey and with different predator and prey densities. Hence, we believe that our novel approach will help many microbiologists to explore bacterial interactions, such as those in predator-prey relationships, and would spawn additional applications that would simplify the study of other unexplored microorganisms on a chip.

## 2.1 Materials and Methods

### 2.1.1 Preparation of the prey, *E. coli* str. MG1655

In this experiment, we used *E. coli* strain MG1655, which is derived from K12 (a wild type strain). A small colony of *E. coli* grown on a Luria broth (LB) agar was inoculated into 5 mL of tryptone broth (TB, 1% tryptone and 0.5% NaCl) media. The *E. coli* cells were then grown in a rotary shacking incubator (32 °C and 200 rpm) to mid-log phase and required about 8 hours for the OD<sub>600</sub> (optical density at 600 nm) reading to be about 0.4. Before the cell motility was observed, cells were centrifuged at 2000×g for 5 min, the supernatant liquid was removed and the pelleted cells were suspended again in fresh (TB) media (30min) and final OD<sub>600</sub> adjusted to a value of 0.5. We also used green fluorescent protein (GFP) as reporter genes by transforming competent MG1655 cells with pLtetO-1, which expresses the GFP gene constitutively.<sup>12</sup>

### 2.1.2 *Bdellovibrio bacteriovorus* culturing techniques

The conventional double-layer agar technique was used for pure cultivation of *B. bacteriovorus* HD100. The cultivating prey was always *E. coli* str. MG1655/pUCDK<sup>29,30</sup>, which was grown at 30 °C and 250 rpm for 12 h prior to starting the predation study or preparing the double-layer plate.

Predators from a well-separated plaque were picked with a flamed loop and transferred to 2 ml of diluted Nutrient broth (DNB, 1/10 NB supplemented by 2 mM CaCl<sub>2</sub>, 3 mM MgCl<sub>2</sub>) in a test tube. To initiate growth of *B. bacteriovorus*, 0.2 ml of the cultivating prey cells were added and this co-culture incubated with shaking at 30 °C until complete lyses of the prey cells occurred, typically 24 h later. This culture was then filtered (0.45 µm pore, Millipore) to remove any remaining prey cells. This filtered sample contained only *B. bacteriovorus* and was again diluted within DNB media and *E. coli* str. MG1655/pUCDK using a prey to predator volume ratio of 2:1.5. After 12 h of co-culturing, the suspension, which had an OD<sub>600</sub> of approximately 0.1, was again filtered (0.45 µm pore) and used directly for the microfluidic experiments. The densities of the filtered samples were measured based on plaque-forming-unit (PFU) that represents the number of free swimming, filterable *B. bacteriovorus* in the sample medium.<sup>31</sup> These samples typically had about 2 × 10<sup>9</sup> predator cells per ml.

### 2.1.3 Microfluidic Concentrator Arrays for Motile Bacterial Cells

The device is composed of a concentrator array at the middle and two gradient generators (mixers) at the top and at the bottom, as shown in Fig. 2.1 (A). First, the concentrator array plays a key role in concentrating motile bacterial cells at each concentrator well and providing many opportunities to observe the predation behaviour of predators toward prey because both predatory and prey microbes are accumulated in circular chambers in 100 µm diameter and 25 µm in height together. Second, the top gradient generator not only introduces microbes uniformly into the concentrator array but it also can produce density gradients of microbes in a controllable manner. For the microfluidic channel design for generating cell density gradients, the Christmas tree structure was utilized in this work.<sup>11</sup> Third, the two gradient generators act as the top gradient generator and they also make it possible to introduce two types of prey microbes into the concentrator array half and half, resulting in two compartmentalized prey or predator concentrations. In addition, they can be used both together and separately for loading microbes into the concentrator as well. We designed and fabricated a 10 by 3 concentrator array to find out averaged predation rates from the three rows as shown in Fig. 2.1(B) and(C). We refer to the location of each concentrator (well) as w<sub>i,j</sub> in a matrix format. The subscript ‘i’ and ‘j’ denote the row and column number, respectively, and the range of ‘i’ is between 1 and 3 and that of ‘j’ is between 1 and 10. For example, the concentrator at the top and the most left is denoted as w<sub>1,1</sub>.

### 2.1.4. Fabrication of the microfluidic devices

We fabricated microfluidic devices using a standard softlithography technique.<sup>32</sup> Briefly, a 20 µm thick SU-8 (Microchem 2025, Newton, MA, USA) master was fabricated and the surface was

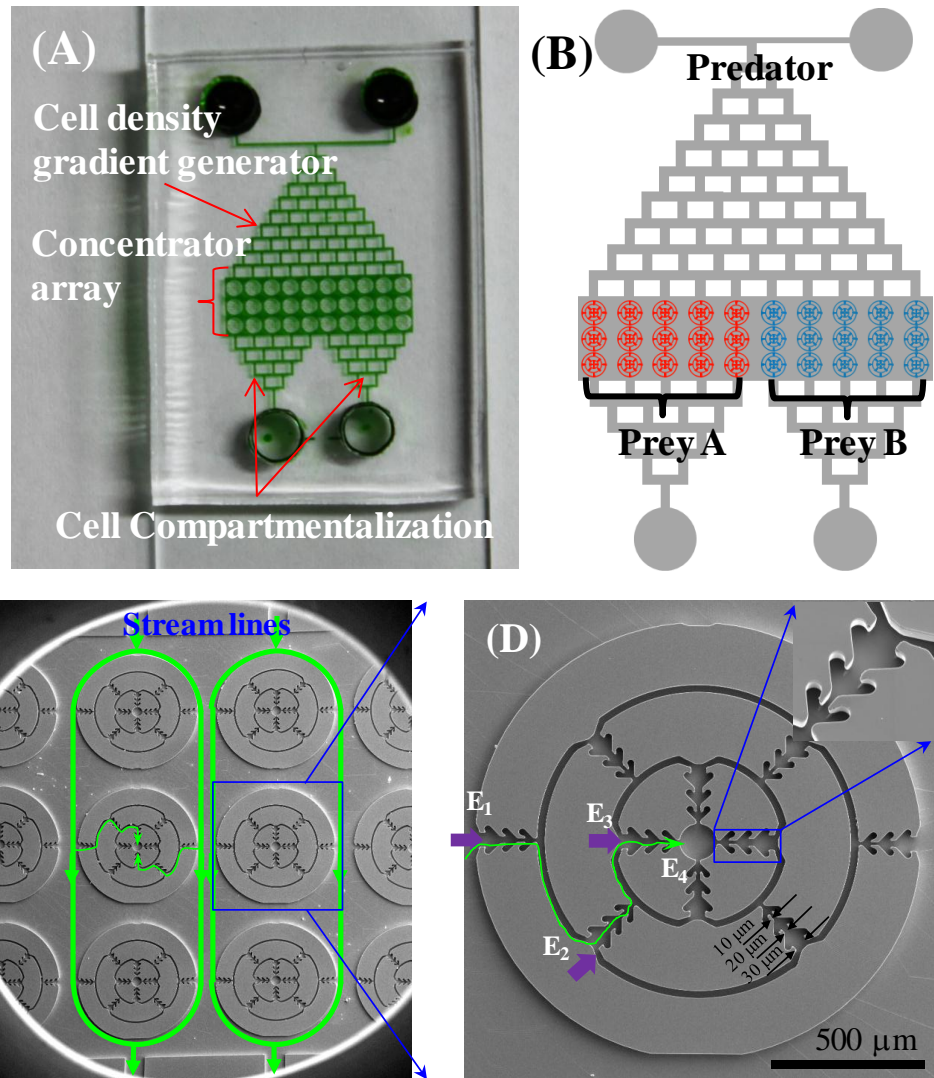


Fig 2.1 Microfluidic concentrator array device. (A) A photograph of the concentrator array device. (B) Schematic of the device consisting of three parts: a 10 by 3 concentrator array, a Christmas tree-shaped microfluidic channel at the top and two separate Christmas tree-shaped channels at the bottom. (C) A SEM image of part of the concentrator array. Since the entrances of the concentrator array are perpendicular to the fluid streamlines, only motile cells can swim out of the stream and enter the concentrators. The green arrows represent the trajectories of cell movements. (D) The arrowhead-shape structures guides cells along the trajectory in green (from E<sub>1</sub> to E<sub>4</sub>) and prevent cells in the centre of the concentrator from escaping. Owing to the symmetrical design and high hydrodynamic resistance of the circular channels connected with arrowhead-shaped channels, any viscous shear stresses caused by flow will have little or no effect on the cells concentrated at the centre of the array (E<sub>4</sub>).

silanized using trichloro (3, 3, 3-trifluoropropyl) silane (Sigma Aldrich, Korea) in a vacuum jar for an hour. Polydimethylsiloxane (PDMS) pre-polymer was then cast, cured and peeled off to prepare the microfluidic devices. The PDMS devices were treated with oxygen plasma under 50 sccm of O<sub>2</sub> and 70 W for 50s (Cute-MP, Femto Science, Korea) prior to the experiments. This treatment was done to make the surfaces of the PDMS channel hydrophilic so that solutions flowed along the channel easily.

### 2.1.5 Experimental procedure and data analysis

All microchannels were washed with a PBS buffer solution to remove impurities and then coated with Pluronic surfactant (F-127, 0.01%) to minimize non-specific binding between the cells and glass surfaces. The residue of the surfactant near the centre of all concentrators was subsequently rinsed with a TB buffer solution (about 200 µl) for about 4 hours. For all experiments, the prey cells were loaded initially and then a constant flow was maintained to allow the motile cells to swim out of the fluid stream and enter the entrance of the concentrator (see green trajectories in Fig. 2.1(D)). Once a cell enters the arrowhead-shaped structure (indicated with E<sub>1</sub> in Fig. 2.1(D)), escape from the structure is minimal since this shape guides the cells toward the next inner ring. In this manner, a cell would be continuously directed toward the centre of the concentrator, for example, along the green trajectory shown (E<sub>2</sub> through E<sub>4</sub>). Since the number of cells in each concentrator (N<sub>total</sub>) increased in a fairly linear manner over time (D<sub>t</sub>), one could possibly control the total number of cell at the concentrator array by adjusting concentration time, i.e., N<sub>total</sub>=F<sub>cell</sub>× D<sub>t</sub>, where F<sub>cell</sub> is a constant concentrating flux of cells. After the prey cells were concentrated at a desired density the excess prey cells within the main channels that enclose the 10 by 3 concentrator array were flushed away with DNB media (otherwise we noted it). Subsequently, the predator cells were loaded and concentrated in the same manner. After the predatory cells were concentrated within the array, any excess cells outside of the concentrators were removed by flushing the channels with additional DNB buffer solution. In 1 hour we stopped the flow and quantified GFP signal from each concentrator. It should also be noted that the concentrator was designed symmetrically and has only two entrances that are perpendicular to the streamline so that the prey cells that were concentrated at the centre of the concentrator prior to addition of the predatory cells were not affected by the fluid motion. We used a fluorescent microscope (Olympus IX71) equipped with a CCD camera (Clara, Andor Tech, CA, USA) and Metamorph 7.7 (MDS Analytical Technologies, Sunnyvale, CA) to photograph phase contrast and fluorescent images of cells. All image processing and quantification of the fluorescent intensities were performed using Metamorph 7.7 and the results were plotted using Origin 8.0 (OriginLab, Northampton, MA, USA).

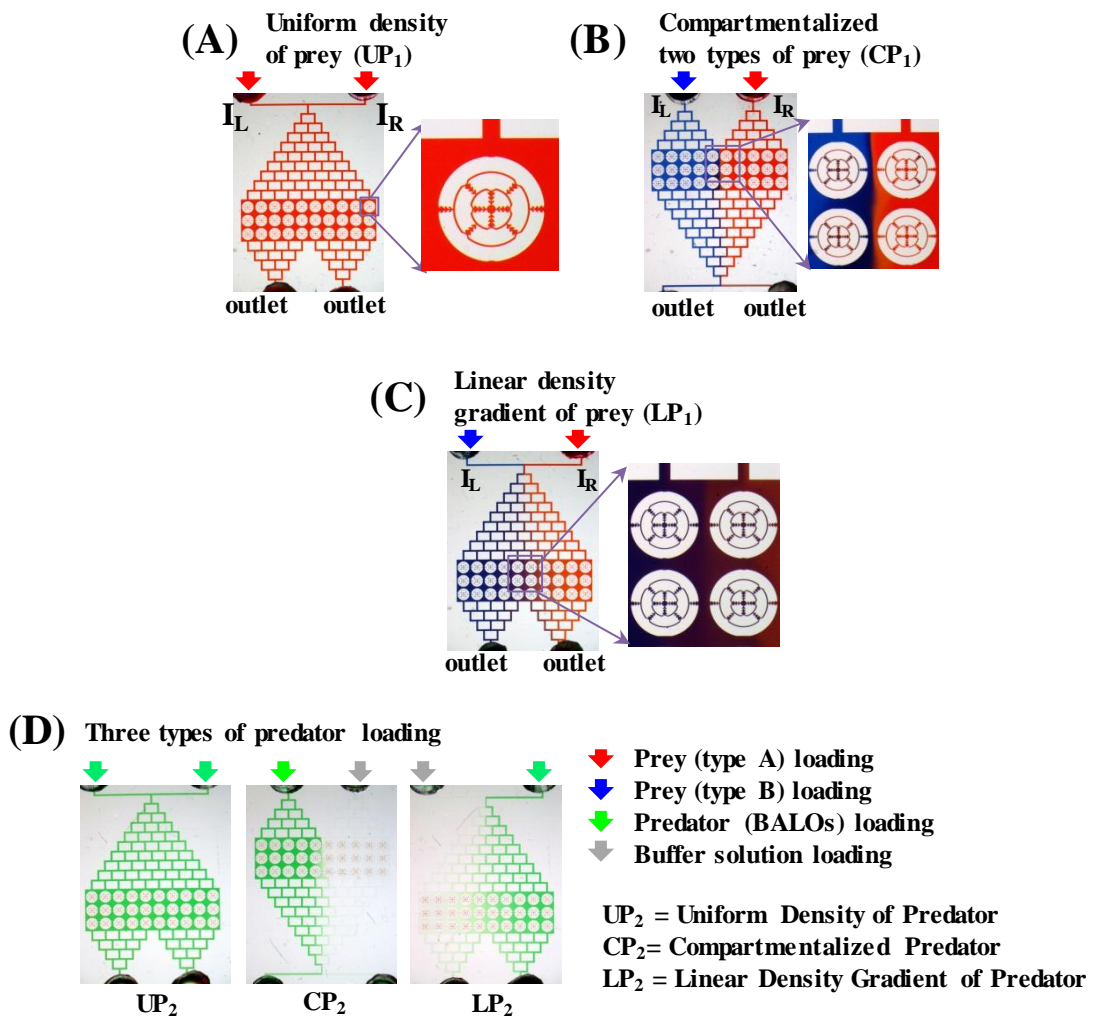


Fig. 2.2 Various experimental configurations tested in this study. (A) Prey cells are loaded through the top channels that contain the same density and suspension volume of prey in both inlets ( $I_L$  and  $I_R$ ) to produce a uniform prey density at the concentrator array. (B) Using the bottom channels, two types of prey cells can be loaded separately and at the same time, resulting in a compartmentalized prey density. (C) Prey cells are loaded by using the top linear density gradient generator channels. (D) Predator cells can be loaded in the same manner: a uniform density, a compartmentalized density and a linear density gradient.

## 2.2. Results and discussion

### 2.2.1 Experimental Configurations for the Concentrator Array

The concentrator array allows various experimental conditions to be tested simultaneously, as shown in Fig. 2.2. To visualize these experimental conditions, food dye solutions were pumped into the array. Both predator and prey cells can be loaded using either of the top or the bottom channels. For example, when prey cells are loaded using both the left (IL) and right reservoirs (IR) from the top channels using the same density and cell suspension volume, the concentrators will have a uniform cell number/density (Fig. 2.2(A)). On the other hand, when a cell suspension is loaded only from the right reservoir (IR) and a buffer solution from the left reservoir (IL) through the bottom channels, the concentrators show a compartmentalized cell density (Fig. 2.2(B)). It is also possible to produce a linear gradient of prey cells along the concentrator array ( $w_{i,j}$  where  $j$  increases) by loading a buffer solution into the left (IL) and a cell suspension into the right reservoir (IR) through the top channels (Fig. 2.2(C)). Sequentially, the predatory cells can be loaded using any of these three formats. Thus, the device permits 9 different experimental conditions to be tested. In this work we combined two different prey conditions with three predator conditions. We changed the prey and the predator conditions such as “uniform density”, “compartmentalized density”, and “linear density gradient” and in this work three experiments that can be referred to as ‘UP<sub>1</sub>UP<sub>2</sub>’, ‘UP<sub>1</sub>CP<sub>2</sub>’, and ‘LP<sub>1</sub>UP<sub>2</sub>’ are utilized as described in Fig. 2.2. Since motile prey and predator cells can be concentrated in a mechanically confined chamber with various experimental conditions, we were encouraged to facilitate the predation behaviour assays by predator cells toward prey cells using the concentrator array device.

### 2.2.2 Concentration of motile microbes

The concentration mechanism has been reported in our previous work.<sup>14</sup> Basically, the microfabricated ratchet structure permits only motile cells to enter the array where the concentrator, which consists of two circular channels connected with arrowhead-shaped structures, guides them into the centre of each concentrator, as shown in Fig. 2.3. The microfluidic channel network, however, was modified so that the two inlets were perpendicular to the streamlines. In doing so, the effects of viscous shear stresses on the cells in the centre of the concentrators were minimized. Another benefit of using perpendicular entries is that only actively motile cells can swim out of the main streamline and enter the concentrators, which resulted in a high-level concentration of the cells (>20×); the swimming velocity of prey cells ranged from 12 μm/s to 20 μm/s in all experiments. After concentrating the prey cells, the cells remaining outside of the concentrator and channels were flushed out of the array and the predatory cells were introduced and concentrated in the same manner.

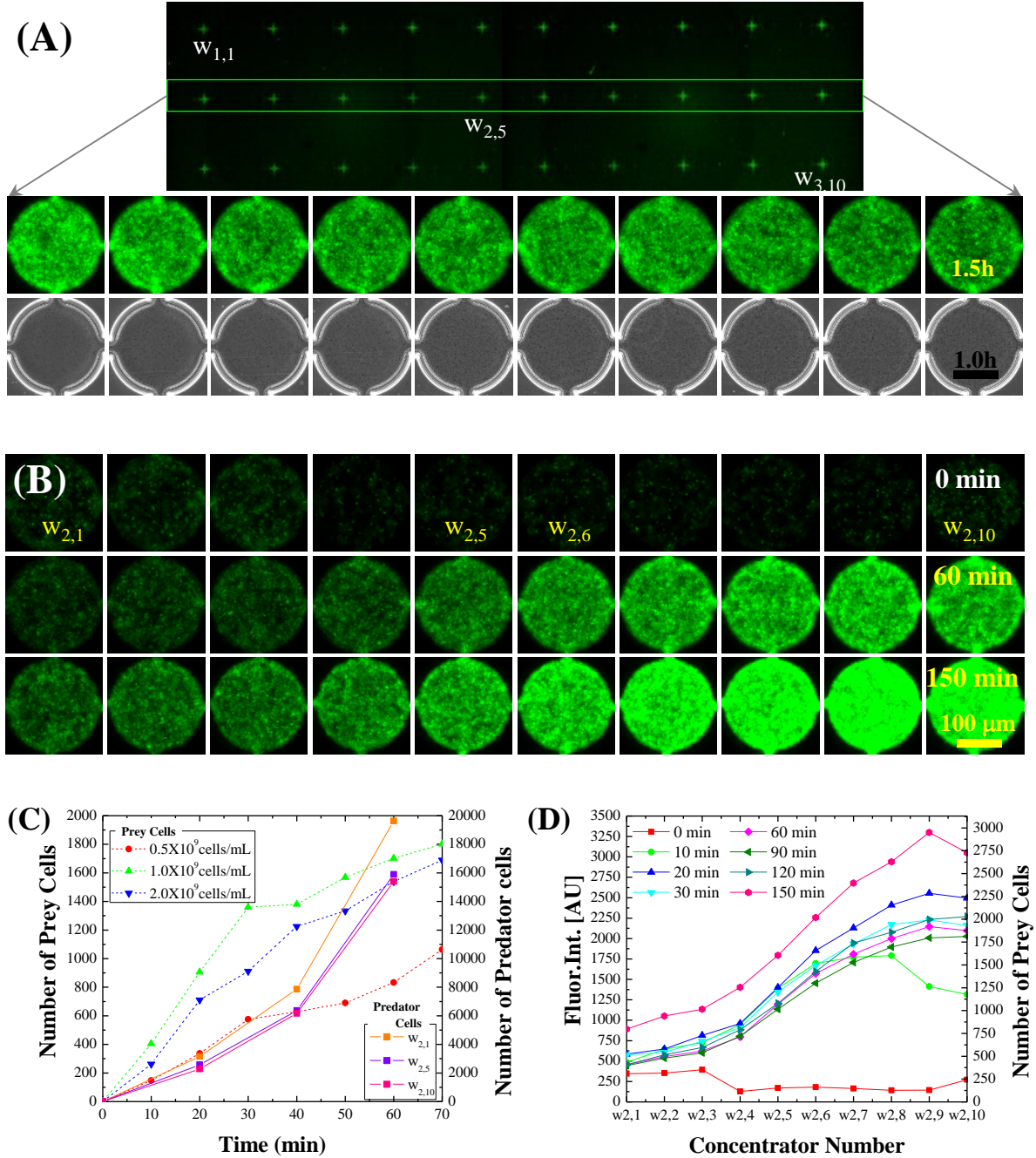


Fig. 2.3 Concentration of predator and prey cells using the 10 by 3 concentrator array. (A) Using a continuous flow of the cell suspensions, motile prey and predator cells are concentrated into the array ( $w_{i,j}$  where  $i=1, 2, 3$  and  $1 \leq j \leq 10$ ) over time. Three prey and one predator ( $8 \times 10^9$  cells/ml) densities are tested. (B) Since the prey cell suspension solution is loaded through the top density gradient generator channel, a linear density gradient is formed along the array. (C) The number of cells concentrated in (A) is proportional to the concentrating time and the initial densities of the cell suspensions. (D) The fluorescent intensities measured in (B) show the density gradient formed and the equivalent number of cells per array over time.

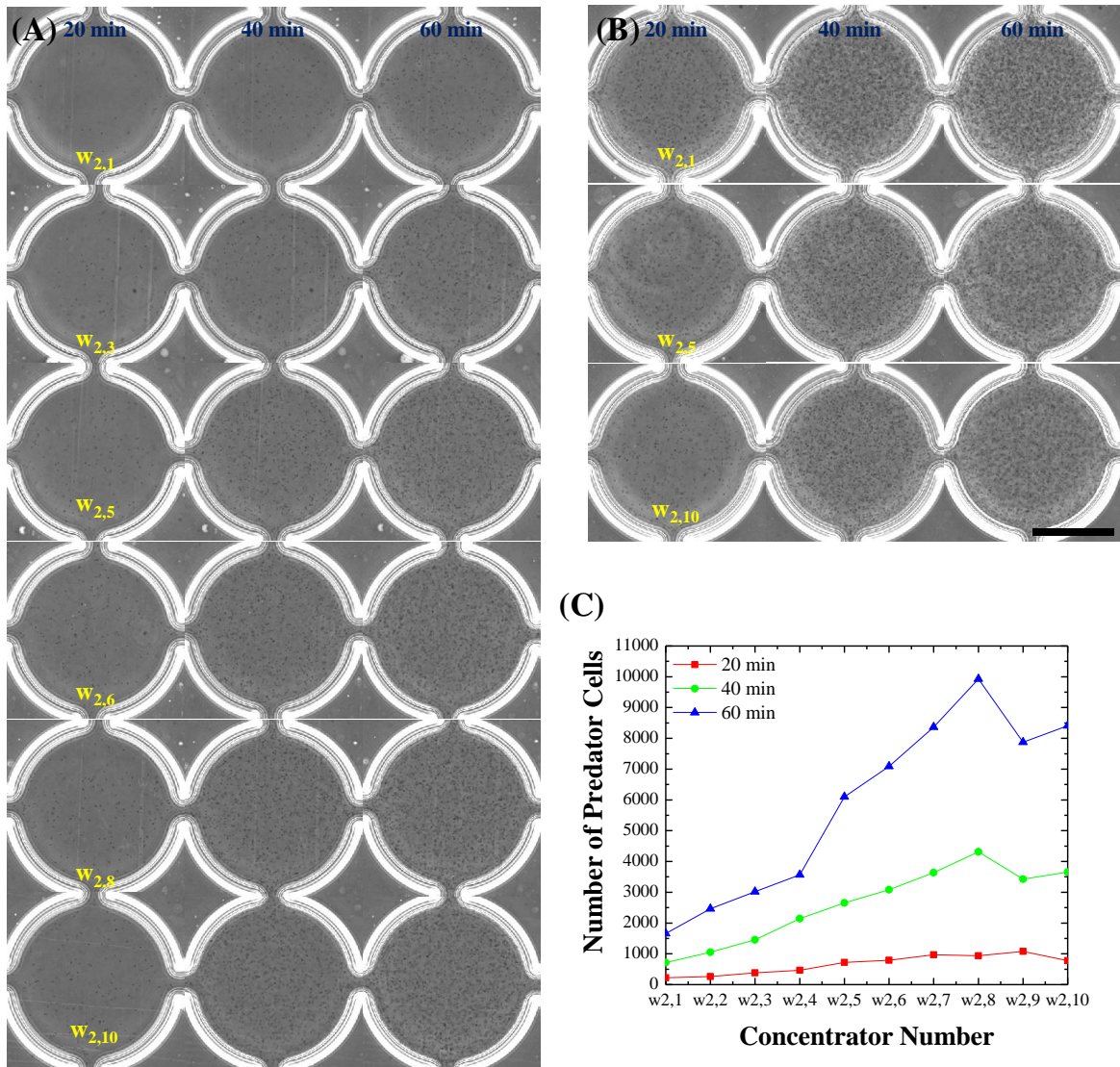


Fig. 2.4 Concentration of predator cells. (A) By applying buffer and predator cell suspension for two different inlets of the device, predator cell concentration gradient can be generated in the device. (B) Uniform concentration of predator cells for each concentrator also possible by applying predator cell suspension on two inlets. The scale bar is 50  $\mu\text{m}$ . (C) Quantification of (A). After 60 minutes, the number of predator cells in the chambers shows linear relationship with concentrator number.

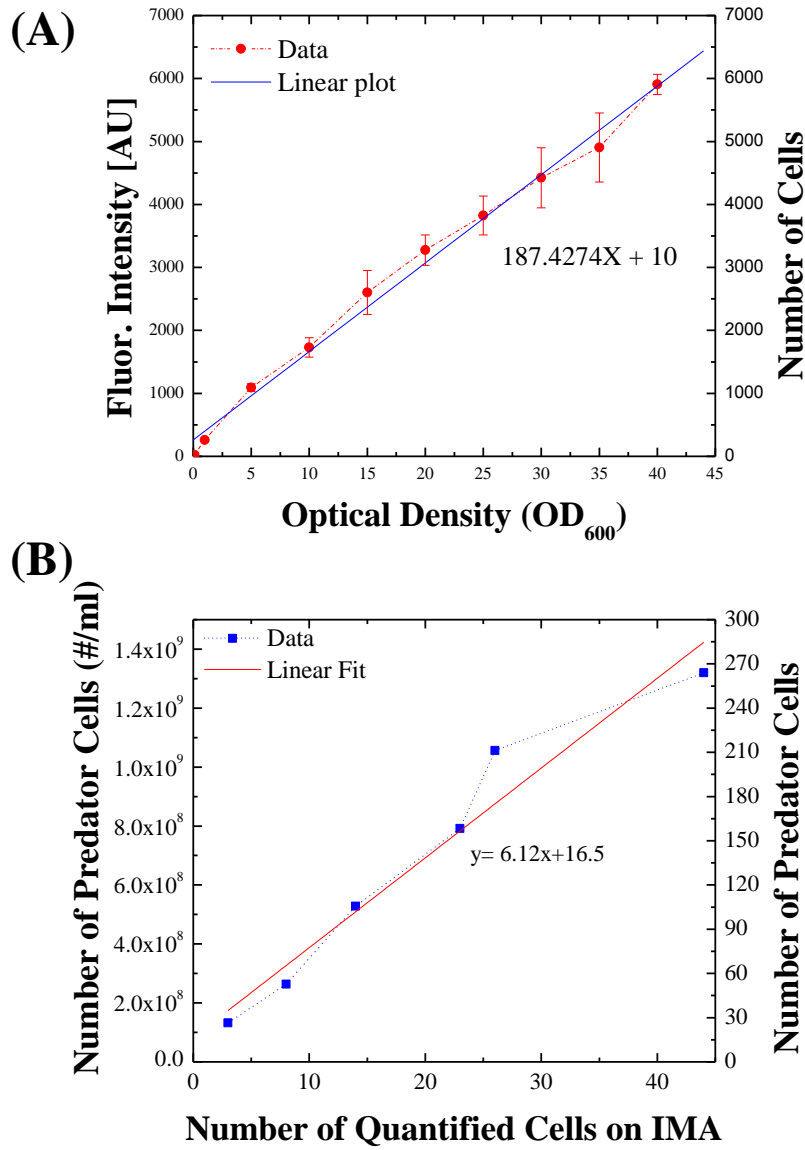


Fig. 2.5 Calibration curve for the calculation of the number of cells in the chamber. (A) The calibration curve between the prey cell density and its corresponding fluorescent intensity. The right y-axis indicates the number of the prey cells in the concentrator in 100 mm diameter. (B) The calibration curve between the predator cell density from the Plaque Forming Unit (PFU) data and its corresponding Image Morphometry Analysis (IMA) values that are obtained from Metamorph software used in this work. The prey and predator cells of which densities/numbers are known were used to fill 25  $\mu\text{m}$  deep microchannels and then fluorescent and phase contrast signals were measured to relate the number/density of cells with the measured signals for the calibration.

Fig. 2.3(A) shows the fluorescent and the phase contrast images of the concentrator array (10 by 3) when the prey and predator cells were concentrated in the array, respectively. Using the fluorescent intensities from the prey cells, which express GFP, and the phase contrast images for the predator cells, the number of cells concentrated in each array was quantitatively analysed over time and under three initial prey cell densities (0.5, 1 and 2 times  $10^9$  cells/ml) and one predator cell suspension density ( $8 \times 10^9$  cells/ml). When cells were loaded through the top gradient generator channel and both reservoirs (IL and IR) contained the same density of cells, the 10 by 3 concentrator array gave uniform fluorescent intensities (Fig. 2.3(A)). In contrast, when a similar loading procedure was used but the left reservoir (IL) was filled with a TB buffer solution without prey, this resulted in a density gradient of the prey cells, as shown in Fig. 2.3(B). Using the concentrator array, we demonstrated that both microbes can be continuously concentrated within the concentrator array regardless of the initial density differences between the inlets. Fig. 2.3(C) and (D) show the quantified results of the concentrated cells that were converted from the fluorescent intensities from the prey and the phase contrast signals from the predator via microscope calibration (see Fig. 2.4 and Fig. 2.5). As a result, we were convinced that a required number of the prey and predator cells can be controlled within each individual concentrator array by adjusting the time because the number of concentrated cells is nearly, linearly proportional to the concentrating time. For the prey cell density gradient, the gradient can be expressed mathematically as  $N_{\text{prey}}(w_{i,j+1}) = kN_{\text{prey}}(w_{i,j})$ , where  $N_{\text{prey}}(w_{i,j})$  is the number of the prey cells at  $w_{i,j}$  and the slope  $k=1.3$  where  $i=1, 2, 3$  and  $1 \leq j \leq 9$ . For experiments, the number of the prey cells can be easily calculated by converting the fluorescent intensities from each concentrator based on the calibration data while that of predatory cells cannot be directly calculated in the presence of the prey cells because of the optical interference in phase contrast images between the prey and the predatory cells. For this reason, in this study, we used the calibration data of the predatory cells obtained in the absence of prey cells to estimate the total number of predatory cells for the experiment (in the presence of prey cells) although the method may cause some degree of uncertainty.

### 2.2.3 Predation of prey (*E. coli*) at a single cell level

First of all, we used the concentrator array device in observing the predation of a single prey cell because the prey and predator cells can be collected within but not escape from the concentrators. This is a unique advantage of the device that allows the predator to easily capture the prey. Using phase contrast and fluorescent microscopy, Fig. 2.6(A) shows several samples during the predation process. The phase contrast image shows both the prey (*E. coli*) and predator (*B. bacteriovorus*) but only the prey is seen within the fluorescent image since the *E. coli* cell constitutively expresses GFP. The GFP signals remain almost constant for 4 hours and then significantly decrease within 30 minutes. This result can be described by the phenomenon referred to as a bdelloplast.<sup>29</sup> As shown in Fig. 2.6(C)

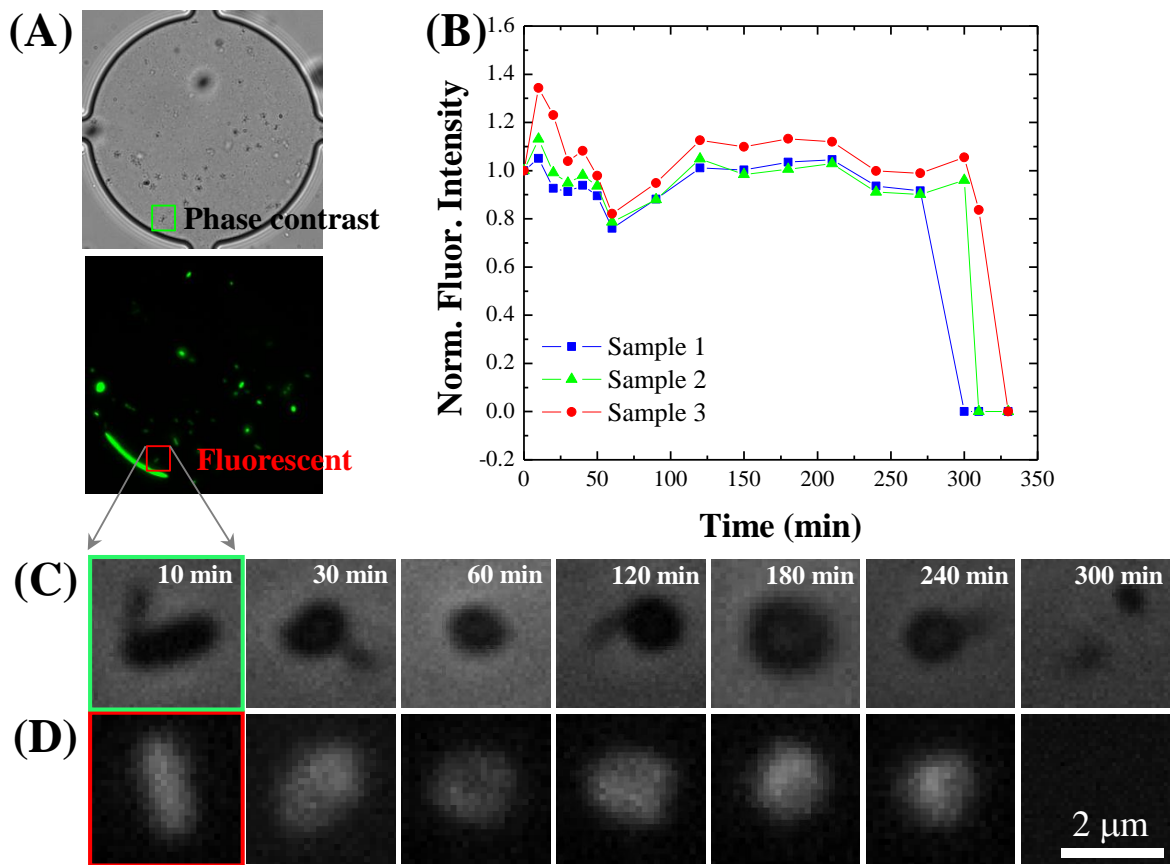


Fig. 2.6 The concentrator array facilitates the observation of the predation at a single cell level because the prey and predator cells are physically confined in the concentrator. (A) A phase contrast image and (B) its fluorescent graph. (C) Show the predation of an *E. coli* by a BALO. The bright light image shows BALO and *E. coli*. (D) The *E. coli* cell constitutively expresses GFP so that it is also seen under a fluorescence microscope but BALO cell is not. A BALO attaches to, penetrates into, modifies the membrane of and then changes the shape of the prey cell. This process is called a bdelloplast during which GFP intensities from the prey cell gradually decrease after about 4 hours because the predator inside the prey digests cytoplasm.

and (D), the BALO attaches to, penetrates into and then changes the shape of the prey cell to a sphere (no lysis). After consuming the entire cytoplasm, the BALO proliferates within the prey cell membrane and then a few BALOs come out from the prey by rupturing the membrane (lysis) which causes GFP to degrade and diffuse away.<sup>30</sup> The predation proceeds for about 4 hours and one prey (*E. coli*) is predated by only one predator (BALO) at a time. This result is in a good agreement with the other literature reporting that the predation typically takes about 4–5 hours<sup>33</sup> although this time can be affected by harsh nutrient and/or prey conditions as reported in other work.<sup>34,35</sup> Here, we note that the device was proven to facilitate predation studies at the single cell level and the result was used for estimating the predation cycle in the following multi-cell assays.

## 2.2.4 Predation of prey by predator at a multi-cell level

### 2.2.4.1 Uniform density of prey and uniform density of predator (UP<sub>1</sub>UP<sub>2</sub>)

We applied the device to multi-cell assays by loading the same prey cells with a constant concentration density ( $0.5 \times 10^9$  cells/mL) along the rows of the concentration array for 1 hour at the flow velocity ranging from 120 to 150  $\mu\text{m}/\text{s}$ . The number of the prey cells amounted to about 2000 in the concentrator ( $N_{\text{prey}}(w_{i,j})=2000$  where  $i=1, 2, 3$  and  $1 \leq j \leq 10$ ) of which volume is about 200 pL since each concentrator is 100  $\mu\text{m}$  in diameter and 25  $\mu\text{m}$  in height. And then, we replaced the cell suspension in the reservoirs with and flush the entire channels with a fresh buffer solution (DNB). Subsequently, the predator cells ( $2.5 \times 10^9$  Cells/mL) were loaded for 1 hour at the same flow velocity at the prey in a similar manner to generate a constant density along the same rows of the concentrator array and the number of predator cells in the concentrator was estimated to be about 5500 ( $N_{\text{pred}}(w_{i,j})=5500$  where  $i=1, 2, 3$  and  $1 \leq j \leq 10$ ).

After initiating predation, changes in the fluorescent intensities from each concentrator were monitored. Since many prey cells were concentrated in the concentrator array, it was easy to quantify changes in the fluorescent intensity over time and relate them with the predation rate of *B. bacteriovorus* toward *E. coli*. As shown in Fig. 2.7(A), in the absence of a predator, the fluorescent intensities remain constant during the extent of the test although the initially uniformly scattered fluorescent signals (cells) appear to be aggregated in 8 hours. This seems to be caused by inactive motility of the cells over time. Given that the net fluorescent intensities are nearly maintained with time, no additional cell division appears to take place, supporting that the number of the prey cells can be controlled only by the concentrating flux of cells ( $F_{\text{cell}}$ ). In addition, this qualitative result confirms that the prey cells cannot express additional GFP due to changes of culture environment such as the lack of nutrients (from TB to DNB) and pH variation while GFP can last within cells about 9 hours.<sup>36</sup> On the other hand, in the presence of BALOs (Fig. 2.7(B)), the fluorescent intensities appear constant

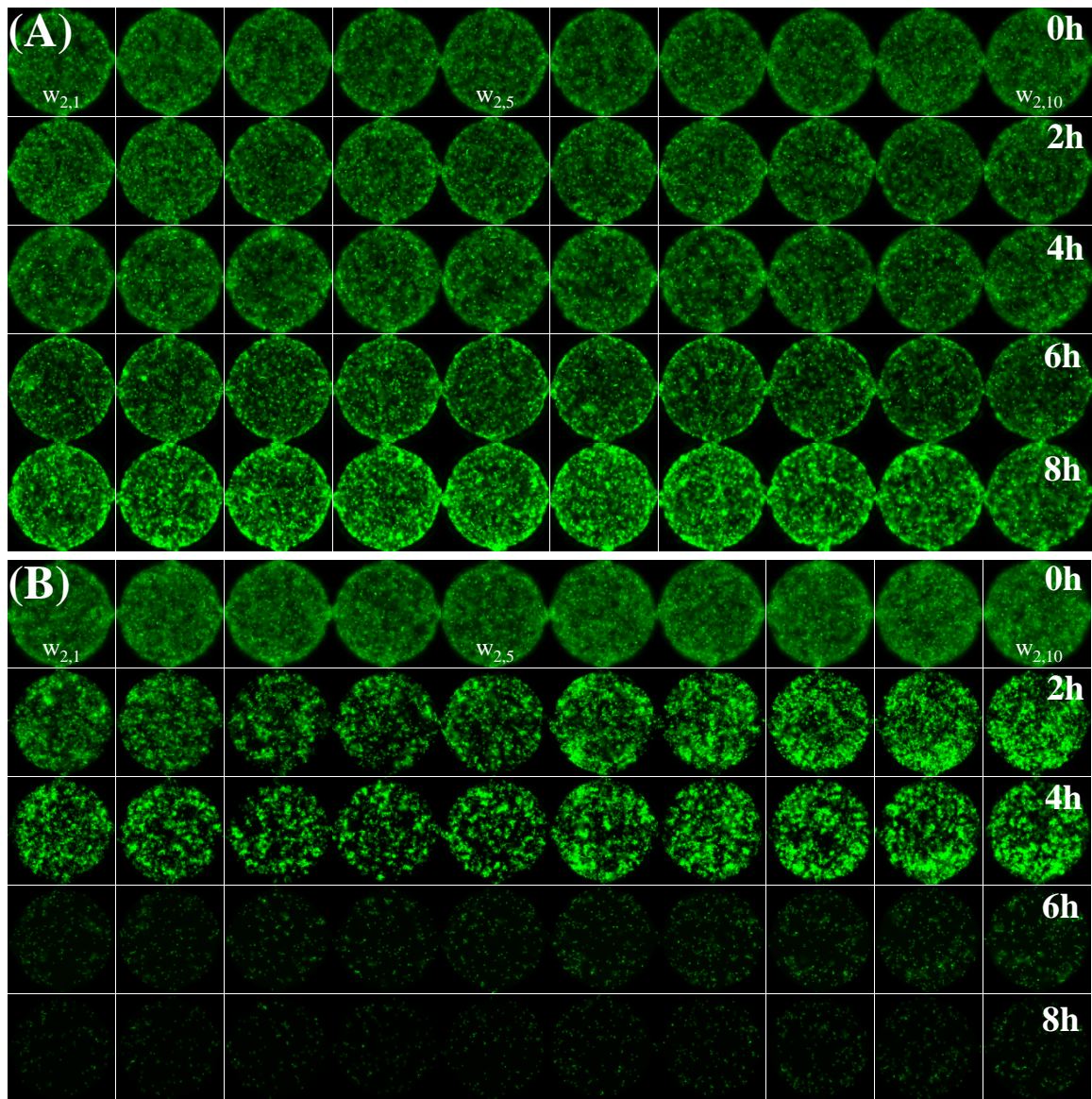


Fig. 2.7 Fluorescence image of control and UP<sub>1</sub>UP<sub>2</sub> experiments. (A) The prey cells are concentrated in the concentrator array for 1 hour, amounting to about 1800 cells in the absence of the predator cells as control. (B) For the predation experiment, the prey cells are concentrated in another device and then predator cells are additionally loaded and concentrated, amounting 2000 and 5500 cells ( $R_{pp}=0.36$ ), respectively. In contrast to the control, the fluorescent intensities start to decrease significantly in 4 hours and almost completely disappear in 8 hours.

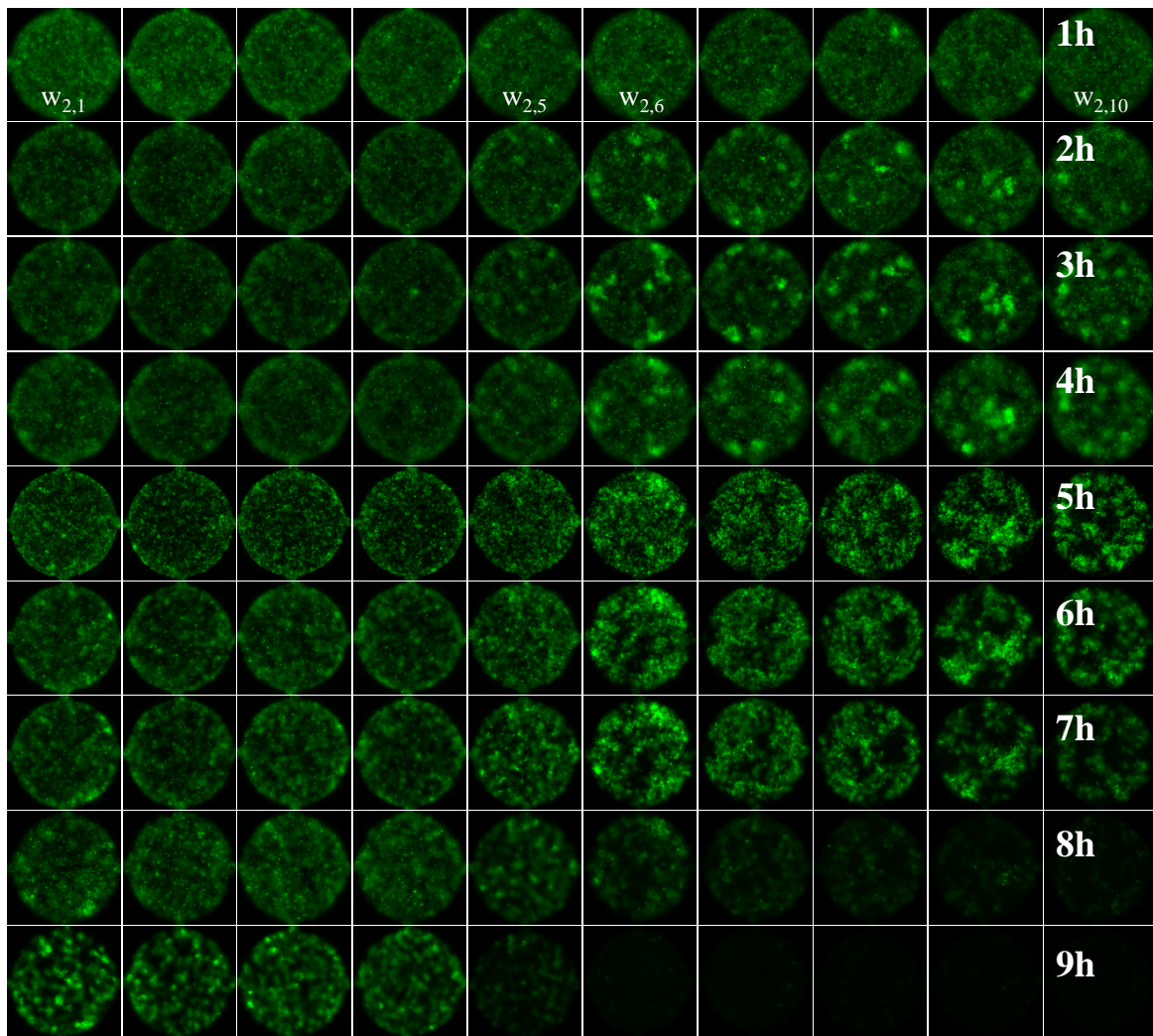


Fig. 2.8 Both control and predation experiments can be performed on a chip. Over uniformly concentrated prey cells (550 cells) for each concentrator, half of the concentrator array was loaded with predator cells (300 cells) and the other half was loaded with TB buffer solution without predator cells, providing both a control and experimental sample on a single chip.

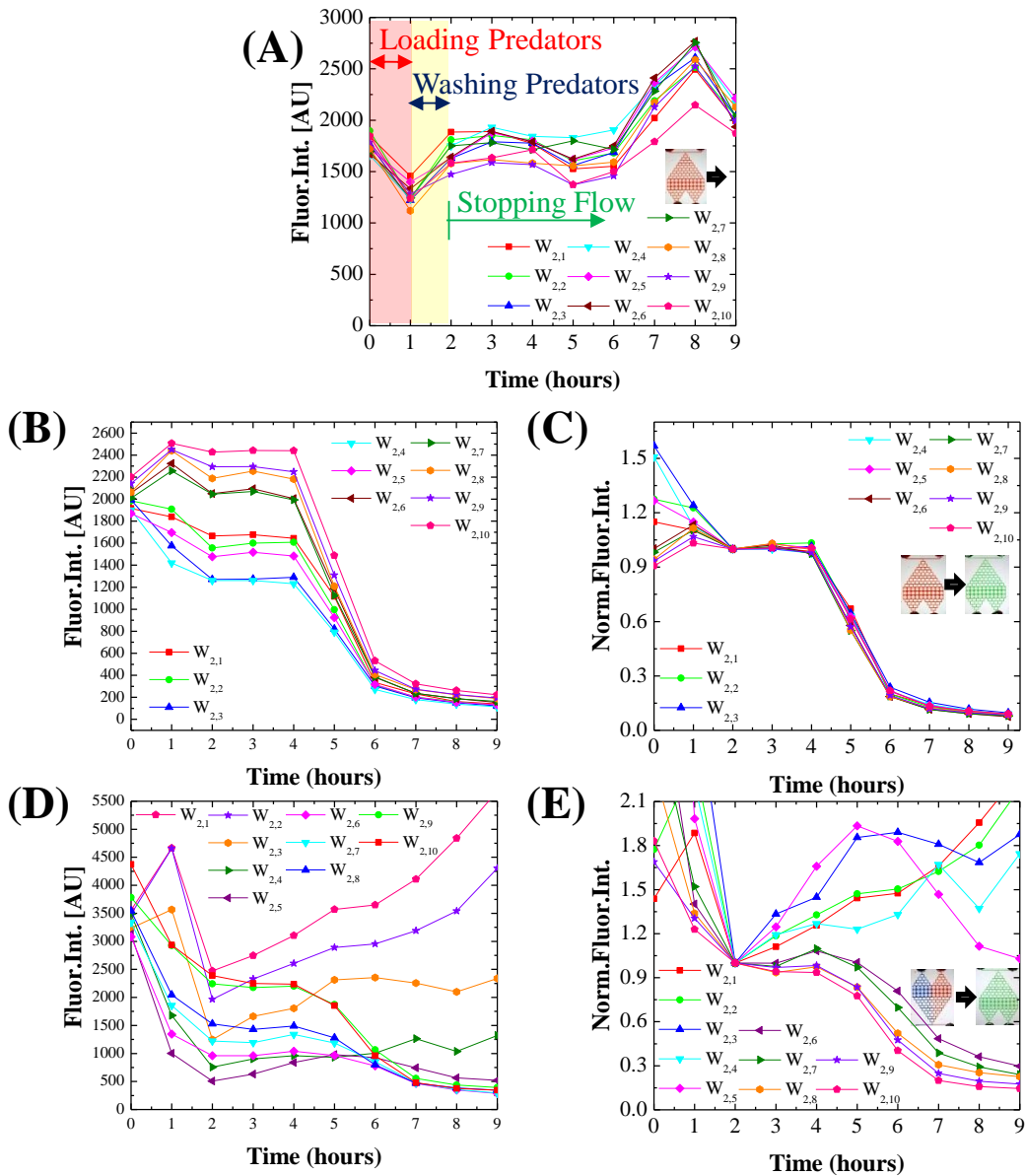


Fig. 2.9 Quantitative analysis of predation and control experiments. (A) Shows the quantification of the fluorescent intensities of the prey cells in Fig.2.7 (A) as control. (B) The fluorescent intensities that are obtained from Fig.2.7 (B). (C) Signals in Fig.2.9 (B) are normalized by the fluorescent intensities at  $t=2$  hours when the infection of the prey cells is completed. In contrary to the control, the fluorescent intensities start to decrease dramatically in 4 hours and then completely disappear in 8 hours because most of the prey cells are continuously predated with time. (D) The fluorescent intensities that are obtained from Fig.2.8. The prey cells are uniformly concentrated (about 3500) for all concentrators but the predator cells are compartmentalized. The half of the concentrators is filled with the predator cells whereas the other half are not so that both the control and predation experiments can be conducted simultaneously on a chip. (E) Signals in Fig.2.9 (D) are normalized by the fluorescent intensities at  $t=2$  hours.

at the early stage (from infection to lysis period,  $t < 4$  hours), start to decrease in 4 hours and then disappear completely in 8 hours. Since the ratio of prey to predator ( $R_{pp}$ ) is about 0.36 (2000 to 5500) all prey cells seem to be infected by the predators within 2 hours; the more the predator cells the faster the infection can be completed. And then, the fluorescent intensities remain almost constant for about 4 hours that is the same duration as the single cell predation (*Bdelloplast*). Interestingly, for the predation experiment, the aggregation of the prey cells appears to take place earlier ( $t=2$  hours) than the control experiment ( $t=8$  hours) and this observation can be described by the motility of the prey cells; the infected prey cells by the predator lose their motility faster, resulting in the non-uniformly aggregated fluorescent intensities in the concentrator array. The lack of motility may cause flagella (25 nm in diameter and 8  $\mu\text{m}$  in length) to be entangled/attached to one another so that this phenomenon may describe the aggregation phenomena observed in the control experiment as well.<sup>13</sup>

Fig. 2.9(A) shows the fluorescent intensities quantified from the prey in the control experiment (Fig. 2.7(A)). The variation of the fluorescent intensities of the prey cells at the early stage ( $t < 2$  hours) seems to be caused by loading the predator cells and washing away the excess of them as depicted in Fig. 2.9 (A). However, in 2 hours, the fluorescent intensities remain almost constant. This is because no predators were loaded and the GFP within the cells are well kept without any degradation, supporting that our approach be appropriate to investigate the quantitative predation assay. In the similar manner, we quantified the fluorescent intensities from the prey in Fig. 2.7(B) and then normalized them with the corresponding fluorescent intensity of each concentrator at  $t=2$  hours (i.e.,  $N_{\text{prey}}(w_{i,j}, t)/N_{\text{prey}}(w_{i,j}, 2)$ ) because we hypothesized that once all the prey cells were completely infected within 2 hours (the  $R_{pp} < 1$ ) they experienced the same predation cycle; the prey cells were observed to be completed infected although the infection time may slightly differ. In addition, in 2 hours, convective flow was stopped to minimize any effects of fluid on the concentrated cells and the predation process. As shown in Fig. 2.9 (A), the normalized fluorescent intensities show a very similar decaying tendency in 2 hours, verifying our hypothesis. In fact, the normalized fluorescent intensities indicate the portion of the infected prey cells out of the total prey cells. In this experiment, 100 % of the prey cells were infected and predated at time. The more the predators and the less the preys, the faster the infection can be completed in the concentrator. This result is well consistent with the qualitative results in Fig. 2.7(A) and (B). From this UP<sub>1</sub>UP<sub>2</sub> experiment, it is noted that this approach has a high potential to be used to characterize the predation rate by predator cells toward prey cells with a wide range of initial prey to predator ratios on a chip (refer to UP<sub>1</sub>LP<sub>2</sub> and LP<sub>1</sub>UP<sub>2</sub>)

#### **2.2.4.2 Uniform density of prey and compartmentalization of predator (UP<sub>1</sub>CP<sub>2</sub>)**

We conducted another experiment by uniformly concentrating the prey cells in the concentrator array ( $N_{\text{prey}}(w_{i,j})=550$  where  $i=1, 2, 3$  and  $1 \leq j \leq 10$ ) while compartmentalizing the predatory cells

( $N_{\text{pred}}(w_{i,j})=0$  where  $1 \leq j \leq 5$  and  $N_{\text{pred}}(w_{i,j})=6600$  where  $6 \leq j \leq 10$  for  $i=1, 2, 3$ ) using the same device, as shown in Fig 2.8(A). Since the half of the concentrator array was filled with the predatory cells whereas the other half was not, this experimental condition allowed performing both the control and UP<sub>1</sub>UP<sub>2</sub> experiment simultaneously on a chip. The result was quite similar to the separate control and predation experiment as demonstrated in Figure 2.7(A) and (B). In the same manner, we normalized the fluorescent intensities and plotted them in Fig. 2.9(C). The fluorescent intensities of the concentrators  $w_{i,j}$ , where  $i=1, 2, 3$  and  $1 \leq j \leq 5$ , remain almost constant whereas those of the concentrators  $w_{i,j}$  where  $i=1, 2, 3$  and  $6 \leq j \leq 10$  decrease significantly about 90% in 9 hours. This result is quite well consistent with the previous experiments shown in Figure 2.9(A) and (B). Here, we note that the device can present both control and experiment results together on a single chip. In addition, this demonstration supports that the microfluidic concentrator array device is very versatile and has a unique advantage over conventional bench-top experiments depending on microplates because it allows precise ratio control and high throughput predation assays.

#### **2.2.4.3 Uniform density of prey and linear density gradient of predator (UP<sub>1</sub>LP<sub>2</sub>) and linear density gradient of prey and uniform density of predator (LP<sub>1</sub>UP<sub>2</sub>)**

Furthermore, we performed another set of experiments using a uniform density of the prey cells in the all concentrator ( $N_{\text{prey}}(w_{i,j})=7000$ ) but a linear density gradient of predator cells ( $N_{\text{pred}}(w_{i,j+1})=kN_{\text{pred}}(w_{i,j})$  and  $N_{\text{pred}}(w_{i,1})=1600$  where  $k=1.2$ ,  $i=1,2,3$  and  $1 \leq j \leq 9$ ). This results in  $0.85 \leq R_{\text{pp}} \leq 4.4$  so that the predation experiment with a wide range of the  $R_{\text{pp}}$  can be conducted on a chip, as shown in Fig. 2.10. For the  $R_{\text{pp}} < 1$  ( $j \geq 6$ ), the fluorescent intensities that were normalized in the same manner as the UP<sub>1</sub>UP<sub>2</sub> experiment, all the prey cells are infected by the predator cells and then experience the same predation cycle over time so that they show almost the same decaying tendency. On the other hand, for the  $R_{\text{pp}} > 1$  ( $j \leq 5$ ), the normalized fluorescent intensities are not overlapped with each other. Instead, they are much greater than those of the  $R_{\text{pp}} < 1$  and decrease slowly and gradually with time in a different fashion. This is because the prey cells were not infected by the predator at a time and the predation cycles take place more than two times. The higher the  $R_{\text{pp}}$ , the greater the normalized fluorescent intensities are obtained, implying that there were still prey cells that were not infected by the predator cells. For example, the  $R_{\text{pp}}$  is nearly 1 for the  $w_{2,6}$  so that the fluorescent intensities start to disappear in 4 hours at which the first predation cycle may be completed ( $t < 5$  hours). In contrast, for the  $w_{2,1}$ , the  $R_{\text{pp}}$  is nearly 4.4 so that the fluorescent intensities do not approach to zero. Apparently after the first predation cycles ( $t < 5$  hours), the second and/or the third predation can occur repeatedly until all the prey cells are consumed.

To confirm this experimental result and demonstrate the device that can provide another experimental condition, we repeated LP<sub>1</sub>UP<sub>2</sub> experiment for a low range of the  $R_{\text{pp}}$  (see Fig. 2.11); the

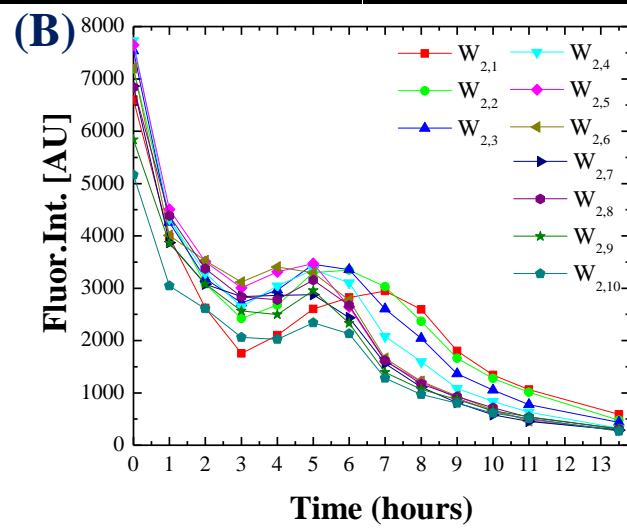
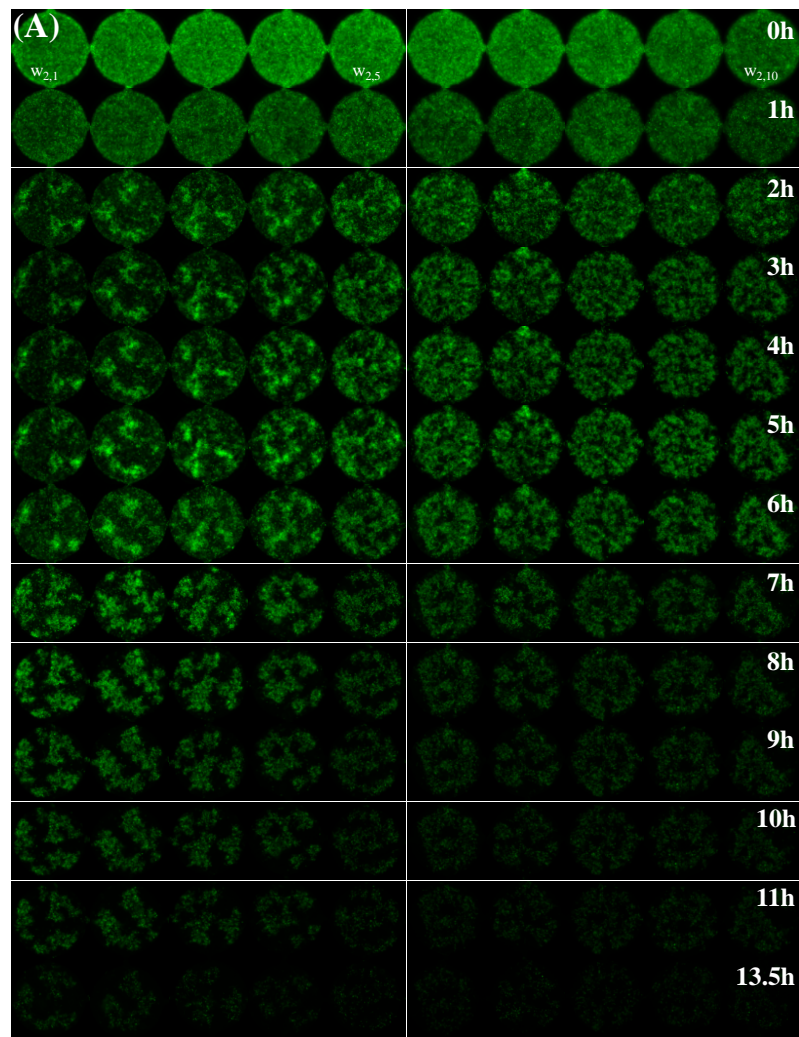


Fig. 2.10. Results of UP<sub>1</sub>LP<sub>2</sub> experiments. (A) Qualitative experimental results. (B) Quantification of the qualitative fluorescence intensities in (A). ( $N_{\text{prey}}(w_{i,j})=7000$  where  $i=1,2,3$  and  $1 \leq j \leq 10$ ) while the predator cells are concentrated with a linear density gradient;  $N_{\text{pred}}(w_{i,j+1})=kN_{\text{pred}}(w_{i,j})$  and  $N_{\text{pred}}(w_{i,1})=1600$  where  $k=1.2$ ,  $i=1,2,3$  and  $1 \leq j \leq 9$ .

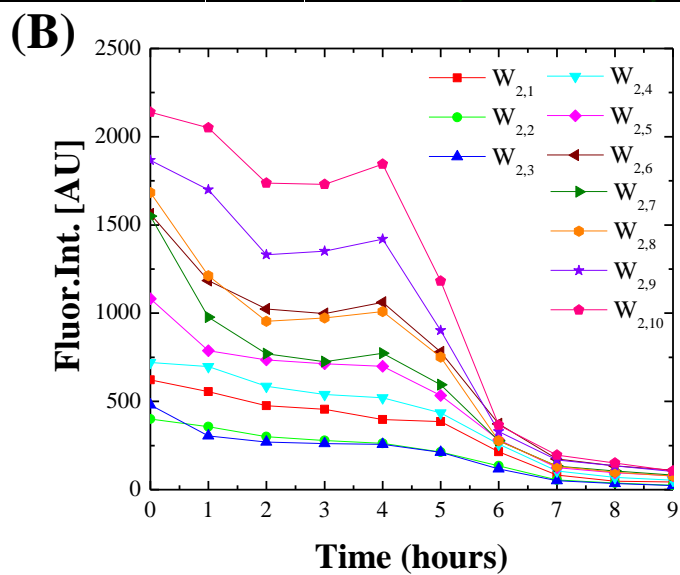
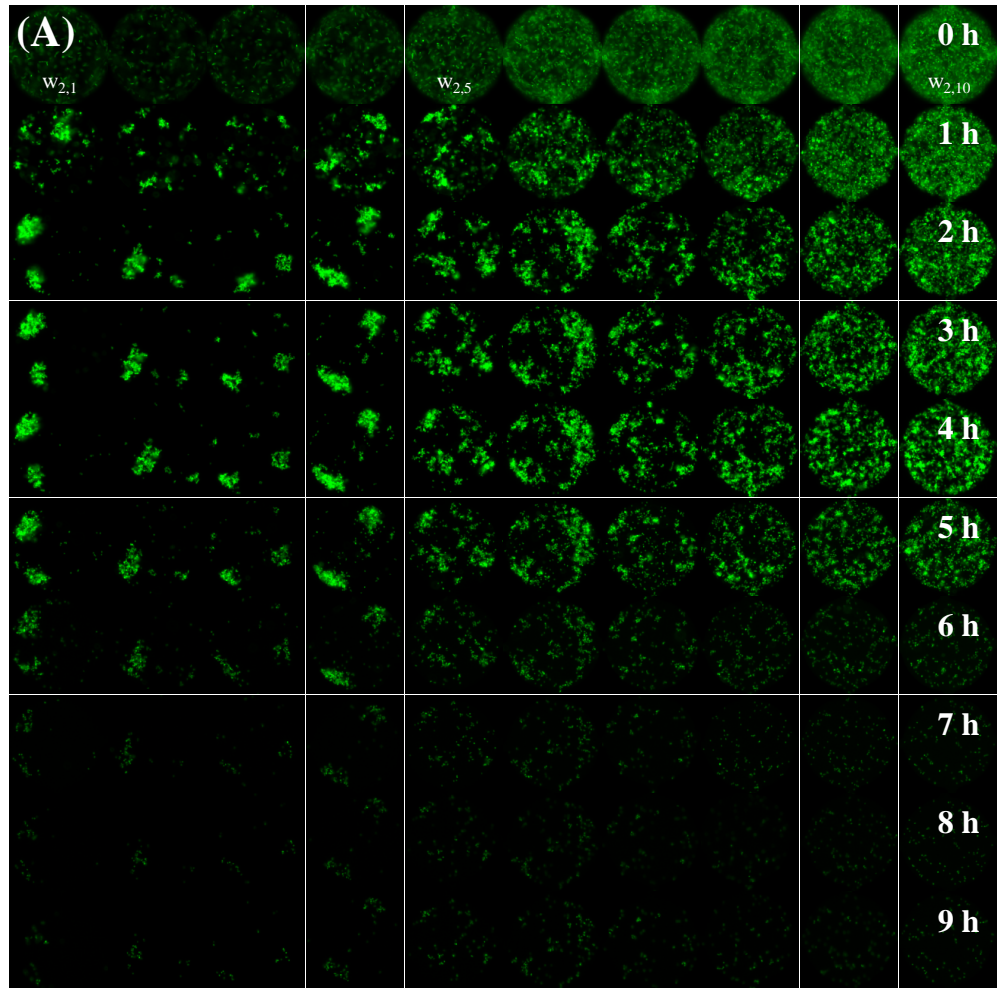


Fig. 2.11 Results of LP<sub>1</sub>UP<sub>2</sub> experiments. (A) Qualitative experimental results. (B) Quantification of the qualitative fluorescence intensities in (A) (i.e.,  $N_{\text{prey}}(w_{i,1})=200$  and  $N_{\text{prey}}(w_{i,j+1})=kN_{\text{prey}}(w_{i,j})$  where  $k=1.3$ ,  $i=1,2,3$  and  $1 \leq j \leq 10$  while  $N_{\text{pred}}(w_{i,j})=5000$  where  $i=1,2,3$  and  $1 \leq j \leq 10$ ). The  $R_{\text{pp}}$  is 0.05 for  $w_{2,1}$  and 0.25 for  $w_{2,10}$ , respectively.

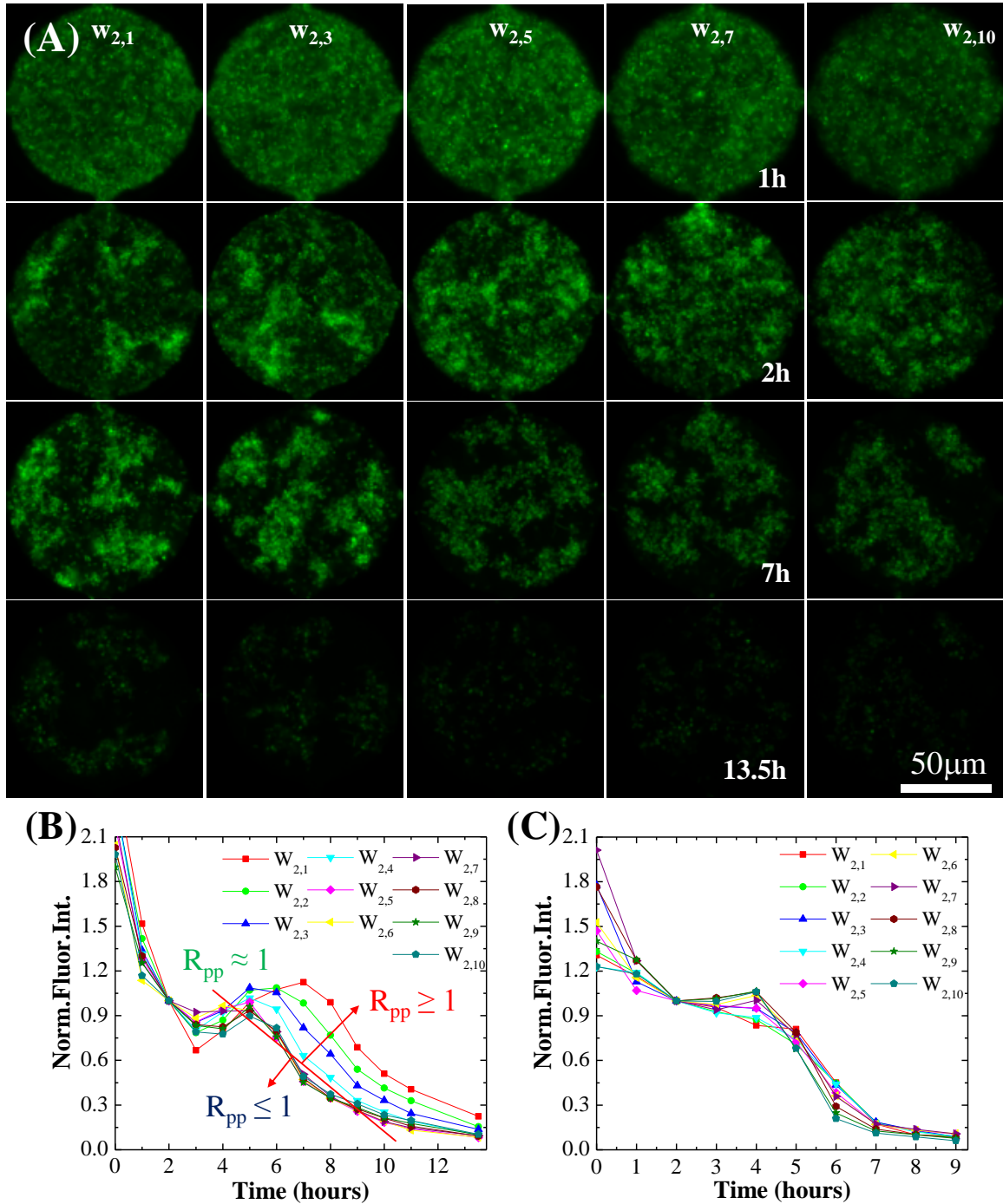


Fig. 2.12 Quantitative results of UP<sub>1</sub>LP<sub>2</sub> and LP1UP2 experiments.(A) The prey cells are concentrated uniformly in the all concentrators (about 7000) while the predator cells are concentrated with a linear density gradient ( $N_{\text{pred}}(w_{i,j+1}) = kN_{\text{pred}}(w_{i,j})$  and  $N_{\text{pred}}(w_{i,1}) = 1600$  where  $k=1.2$ ,  $i=1,2,3$  and  $1 \leq j \leq 9$ ) (UP<sub>1</sub>LP<sub>2</sub> experiment,  $0.85 \leq R_{pp} \leq 4.4$ ). (B) The fluorescent intensities are quantified and normalized with the fluorescent intensities obtained at  $t=2$  hours ( $N_{\text{prey}}(w_{i,j}, t)/N_{\text{prey}}(w_{i,j}, 2)$ ). (C) The prey cells are concentrated with a linear density gradient ( $N_{\text{prey}}(w_{i,1}) = 200$  and  $N_{\text{prey}}(w_{i,10}) = 2000$ ) while the predator cells are concentrated uniformly in the all concentrator (about 5000) for a low range of the  $R_{pp}$

experiment ( $LP_1UP_2$ ,  $0.05 \leq R_{pp} \leq 0.25$ ). The  $R_{pp}$  is 0.05 for  $w_{2,1}$  and 0.25 for  $w_{2,10}$ , respectively. more predators the more preys are consumed and the fast predation leads to the fast decease of the fluorescent intensities. As shown in Fig. 2.12(C), the quantified fluorescent intensities normalized in the same manner as before also show a similar decreasing tendency and show a good agreement with Fig. 2.12(B). In other words, the normalized fluorescent intensities of the  $w_{2,1}$  and  $w_{2,10}$  decreased simultaneously because the  $R_{pp}$  is very low ( $0.05 \leq R_{pp} \leq 0.25$ ) for all the concentrators.

In summary, from the quantified results in Fig. 2.12(B) and (C), we can reach the same conclusion that one prey (*E. coli*) is predated by only one predator (*BALO*) at a time as the single cell level assays. There are several inferences. Firstly, in case that the  $R_{pp}$  is close to one, the fluorescent intensity remains constant for about 4 hours (infection period) and then decreases significantly. This means that, since only one predation cycle occurs, fluorescent intensities approach to zero at a time. Secondly, for the low  $R_{pp}$ , the normalized fluorescent intensities appear to be very close to that of  $R_{pp}=1$ . It seems clear that the normalized fluorescent intensities are determined by the prey not by the predator cells so that the slopes of the normalized fluorescent intensities after cell lysis seems to be very similar to those of  $R_{pp}=1$ . In other words, the normalized fluorescent intensities remain constant during the infection period ( $t < 5$ ) and then continuously and significantly decreases to zero since no more prey cell are left. Lastly, for the high  $R_{pp}$ , the fluorescent intensities remains much longer than the predation cycle (4.5 hours), meaning that both the infection and predation periods take longer and the normalized fluorescent intensities still do not approach zero even after more than two predation cycles. Here, it is necessary to note that the infection rate may differ for high and low  $R_{pp}$  because of the multiple attachment of predator to a single prey and density dependent collisions between prey and predator.<sup>29</sup>

### 2.2.5 Further applications of the device

In this work, 4 out of 9 possible experimental combinations ( $UP_1UP_2$ ,  $UP_1CP_2$ ,  $UP_1LP_2$  and  $LP_1UP_2$ ) were demonstrated, but it is ensured that each prey or predator condition can be integrated with other conditions because the design of the device consisting of the mixing and concentrating component can be applied to many microbes if they are actively motile.<sup>37</sup> Therefore, more quantitative predation assays of motile predatory microbes using the same, single design of the device would be also possible. For example, the device can be further applied to other predation assays by not only producing non-linear gradients of prey or predator by modifying the Christmas tree-shaped mixer network but also compartmentalizing or mixing more types of prey or predator by adding more mixer components into the device. Again, it is noted that the microfluidic channel networks would be versatile for various microbial assays and even very useful and compatible to be integrated with other microfluidic systems.

## Chapter III

### Chemotaxis assay

In this work, we applied our novel microfluidic diffusion based gradient generator to study chemotaxis of predatory bacteria, *B.bacteriovorus*. The pioneering study about chemotaxis of *B. bacteriovorus* was done by S.F.Conti and his colleagues from mid 1970s to late 1970s.<sup>38-41</sup> They used conventional method and investigated four types of major suspects that could affect the chemotaxis of the bacteria such as, yeast extract, amino acids, prey itself, and various compounds. Their final paper, in a series of 4 papers, concluded that there is no evidence that *B. bacteriovorus* uses the chemotaxis to locate their prey. In their study, since they used conventional methods<sup>42</sup>, they repeated laborious experiments with various compounds and time consuming quantification such as plaque forming unit (PFU).

Recently, full genome of *B. bacteriovorus* H.D100 discovered<sup>43</sup> and R. Elizabeth Sockett and her colleagues created Methyl-accepting chemotaxis protein (mcp) gene mutants of *B. bacteriovorus* revealed that chemotaxis does affect to locate their prey<sup>44</sup>. Amy M. Rogosky et al. also discovered that there is a preference of predation by *B. bacteriovorus* so that the predator can easily predate one species than another when they exposed multi-species prey environments<sup>45</sup>. Therefore, chemotaxis of predatory bacteria now become more important since these all clues imposed that there is a certain relationship between search of prey and chemotaxis. However, to study chemotaxis, biologist needs to do the same laborious, time consuming experiments that are not so differ from 1970s.

In this study, we will explore how microfluidic concentration gradients generator can be employed to more efficiently measure the propensity of *B. bacteriovorus* to be attracted chemicals or prey cells in comparison to previous methods such as capillary and Boyden chamber assay. At first, we loaded and observed *B.bacteriovorus* cells on the centre of the spoke shape channel while concentration gradients of compounds, prey itself or even the quorum sensing molecules are constructing along the sub channels (200  $\mu\text{m}$ ) branching out from the centre chamber. After the experiments, we quantified the attraction of the bacterial cells by analysing the number of attracted cells using Image Morphometry Analysis (IMA) software. Since our novel microfluidic multi-concentration gradient generator can generate 6 different concentration gradients simultaneously, the laborious repetition can be minimized. In addition, IMA methods can be shorten the time consuming quantification methods. Therefore, we believe our novel microfluidic concentration gradient generator is very useful tool for quantitative chemotaxis study of predatory bacteria, *B.bacteriovorus*.

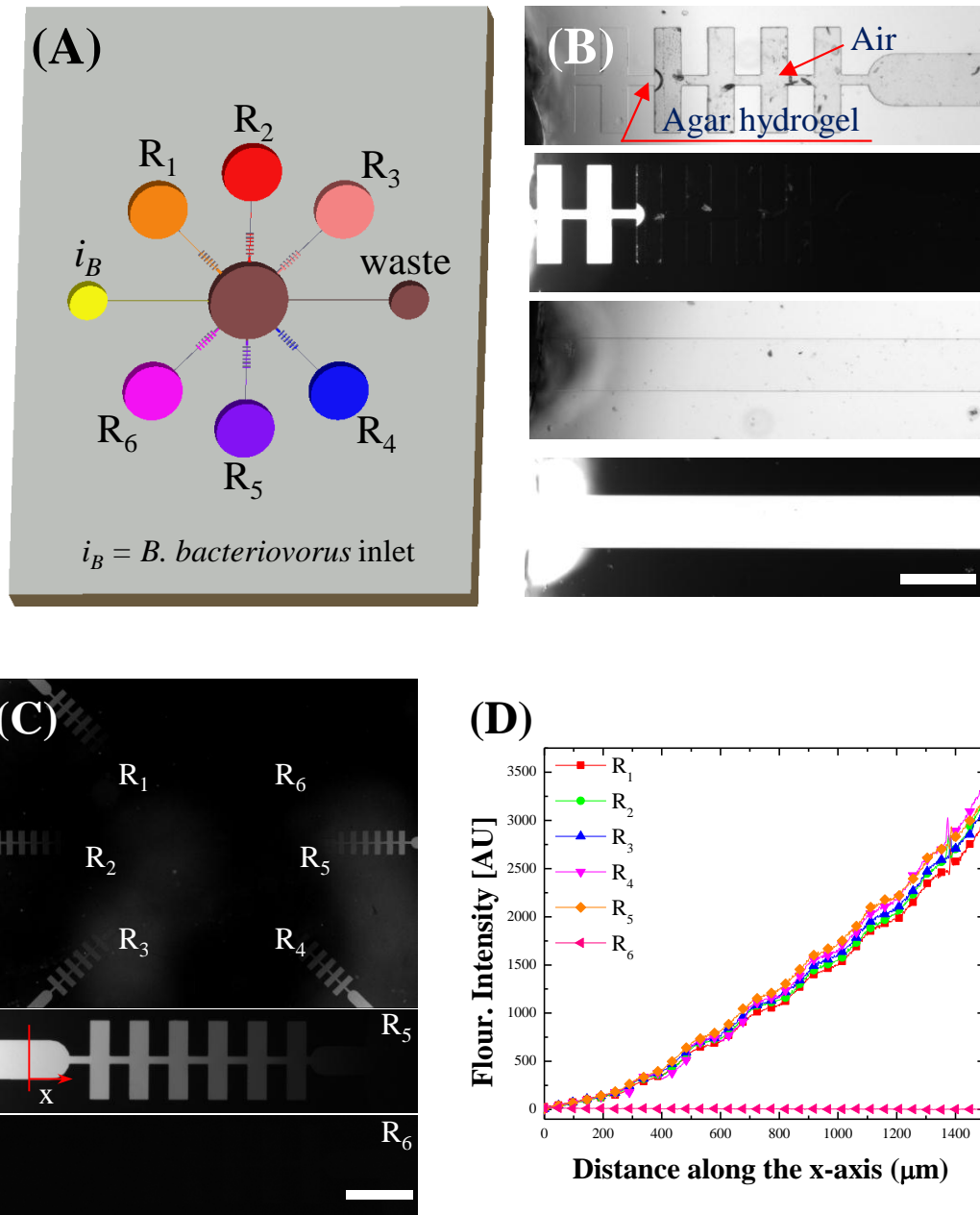


Fig 3.1 Diffusion based microfluidic concentration gradient generator ( $\mu$ CG) (A) Schematic of the  $\mu$ CG device. (B) Effect of H-shape channel on agar plug generation process. Because of H-shape configuration, agarose gel easily solidify and stuck near the loading reservoir while agarose gel flood into the straight channel that has the same channel length and pressure condition . (C) Confirming the concentration gradients of six micro channels (diffusion length  $\sim 300 \mu\text{m}$ ), after 2.5 hours diffusion. (D) The fluorescent signals of six micro channels show stable and robust concentration gradients. Scale bars are 200  $\mu\text{m}$  each.

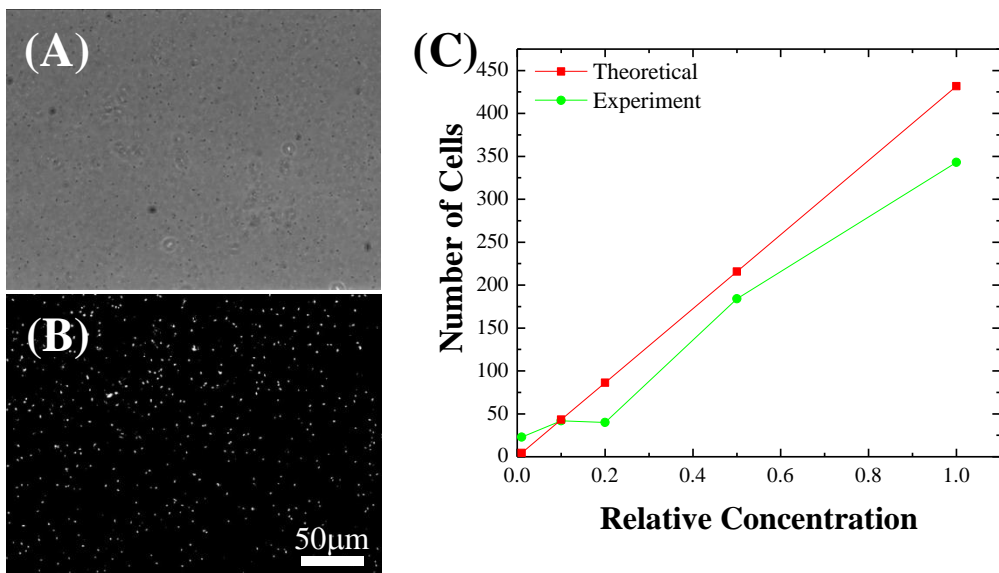


Fig 3.2 The procedure of image analysis of the number of *Bdellovibrio* cells. (A) Bright field image of *Bdellovibrio* cells. Since the size of the cell is too small, quantification is not easy task (B) Use Image Morphometry Analysis (IMA) software, we could change the black dots in (A) to the white dots in (B). The number of cells can be quantified with respect to the number of white dots. (C) The number of cells in the region of interest is proportional to the relative concentration of *Bdellovibrio* cells (1.0 denotes  $4.0 \times 10^9$  cells/ml).

### **3.1 Materials and Methods**

#### **3.1.1 Bacterial strains, materials, and growth media**

The conventional double-layer agar technique was used for pure cultivation of *B. bacteriovorus* H.D.100.<sup>45</sup> The bacteria from a well-separated plaque are picked up with a flamed loop and transferred to 2 ml of diluted Nutrient broth (DNB, 1/10 NB and supplemented by 2mM CaCl<sub>2</sub>, 3mM MgCl<sub>2</sub>) in a test tube. After that, 0.2ml of *E. coli* cells (MG1655 PUCDK strain, 37 °C, 250rpm, 12h incubated) are added and co-cultured in the incubator with shaking at 30°C until complete lyses of prey cells has occurred approximately 24h later. Suspension of pure *B.bacteriovorus* filtered (0.45μm pore, Millipore) to get rid of remained debris and inoculated again to DNB media so that the volume ratio of prey and predator is 2:1.5. After another 12h co-culture of prey and predator, the suspension was filtered (0.45μm pore, Millipore) at the final OD<sub>600</sub> approximately 0.1.

#### **3.1.2 Fabrication of microfluidic device**

We fabricated microfluidic devices by means of standard softlithography technique <sup>32</sup>. Briefly, a SU-8 (Microchem 2025, Newton, MA, USA) master approximately 20 μm thick was fabricated using standard photolithographic procedures. The surface was silanized using trichloro (3, 3, 3-trifluoropropyl) silane (Sigma Aldrich, Korea) in a vacuum jar for an hour. Polydimethylsiloxane (PDMS) was then cast, cured and peeled to prepare the microfluidic devices. The PDMS devices were treated with oxygen plasma under 30 sccm of O<sub>2</sub> and 70W for 8s and bonded with a glass substrate prior to the experiments (see, Fig. 3.1 (A)).

#### **3.1.3 Construction of hydrogel plugs in micro channels**

The hydrogel plugging method used to construct chemical gradients in a microfluidic device.<sup>12</sup> About 5 μl of agarose solution at 65°C was loaded at each reservoir after partially exposed the oxygen plasma in a micro channel. The loaded gel solidified near reservoirs due to the temperature shift on the H-shaped structure (see Fig. 3.1 (B)), and the position of a hydrogel plug in a micro channel can be controlled by adjusting time of oxygen plasma treatment. The travel length of agarose solution was proportional to the time that we exposed oxygen plasma to the device. Repeated narrow and wide channel in H-shaped structure accelerates temperature shift. The transition of the surface property from hydrophilic to hydrophobic and the temperature shift due to the geometry are the major issues of the gel structure construction in a microfluidic channel. After constructing the hydrogel plug, we characterized the concentration gradients to ensure working of the plug by measuring diffused fluorescein isothiocyanate (FITC) signal in the micro channels after 2.5hrs of diffusion (see Fig. 3.1 (C) and (D)).

### 3.1.4 Quantification of chemotaxis using image analysis

All micro channels were coated with Pluronic surfactant (F-127, 0.01%, Sigma Aldrich) to minimize any nonspecific binding between the cells and the glass surface. The residue from the surfactant was subsequently rinsed with culture medium or the motility buffer solution. The cells then were loaded into the micro channels and observed. All bright-field and fluorescent micro-images were obtained with an inverted epi-fluorescent microscope (Olympus, IX-71, Japan) and a CCD camera (Andor, Clara, USA). Images were recorded at 15 fps using 20X and 40X objective lenses. The number of the bacterial cells was analyzed by Image Morphometry Analysis (IMA) in Metamorph software after 1 hour exposed to attractants (see Fig 3.2).

### 3.1.5 Theoretical Analyses

The transient convection-diffusion is governed by the mass balance equation:

$$\frac{\partial C}{\partial t} = -u \nabla C + D \nabla^2 C \quad (1)$$

where  $C$  is the concentration,  $u$  is the velocity of a fluid, and  $D$  is diffusion coefficient of molecules. In the absence of convection flow ( $u=0$ ), diffusion is assumed to be one-dimensional in a microchannel because height of channel is much smaller than length of it ( $H \ll L$ ). Therefore equation (1) reduces

$$\frac{\partial C}{\partial t} = D \frac{\partial^2 C}{\partial x^2} \quad (2)$$

where  $x$  is the direction along the channel.

To solve the equation, we need two boundary conditions and one initial condition. From the knowledge of the geometry and concentration of the reservoirs,

Boundary conditions:  $C_i(0,t) = C_{i0}$  (3)

$$C_i(L,t) = 0 \quad (4)$$

Initial conditions:  $C_i(x,0) = 0$  (5)

With these boundary and initial conditions, the equation (2) can be solved and the solution is given by a complementary error function,

$$C_i(x,t) = C_{i0} \left[ 1 - \operatorname{erf} \left( \frac{L-x}{2\sqrt{Dt}} \right) \right] \quad (6)$$

at steady state,

$$C_i(x, \infty) = -\frac{c_{i0}}{L}x + C_{i0} \quad (7)$$

Therefore, the concentration gradients are theoretically asymptotic with time and the gradients of small molecules gradually become linear. To maintain boundary conditions, centre chamber of the device should be continuously flushed with culture media or cell suspension.

## 3.2. Results and discussion

### 3.2.1 Chemotaxis towards yeast extract

We investigated the chemotaxis of *Bdellovibrio* cells (HD 100 strain) in our novel multi-concentration gradient generator with various concentration of yeast extract which is a well-known chemoattractant for predatory bacterial cells.<sup>39</sup> DNB medium samples (40 µL) containing 0 % (R1), 0.001 % (R6), 0.01 % (R2), 0.1% (R5), 1% (R3), and 5 % (R4) of yeast extract were added to the reservoirs, as shown in Figure 3.3 (A). We flushed cell suspending medium continuously from inlet to outlet during the experiments to maintain boundary conditions, in other words to minimize cross-contamination via diffusion.

Fig. 3.3 (C) shows the accumulation of *B.bacteriovorus* strain HD 100 inside of microfluidic channel when the cells exposed to the concentration gradients after 1hr. We set the region of interest inside of the H-shaped channel, because the region is good for minimize accumulation of *B.bacteriovorus* cells by its fast and random motility. The area of R.O.I is  $160 \times 80 \mu\text{m}^2$ . At the beginning of the experiment, the number of cells within R.O.I was nearly the same for all concentrations. After 60 minutes, the number of attracted cells was apparently different with respect to the concentration of yeast extract. The higher concentration shows the more cells attracted. We quantified the attracted cells within R.O.I using IMA software.

In figure 3.3 (D) and (E) show the results. R.N.A.C refers to the relative number of attracted cells (RNAC = number of attracted cells in the test channel / number of attracted cells in control channel). The concentrations below 0.01% show no attraction compared with control medium. Usually, bacterial cells show chemotactic behaviour over certain threshold concentration.<sup>46</sup> When the cell exposed to too low concentration or concentration gradients, cell may not sense the molecules or gradients (see Fig 3.3 (B)). On the other hands, when the cell exposed to too high concentration, cell may not grow or survive since too high concentration of attractant become toxic to cells.

For yeast extract, threshold concentration for HD 100 strain is 0.1% and the maximum attraction occurs at 1% of initial concentration of yeast extract (The concentration of R.O.I is nearly 0.3%, as shown in Fig. 3.3(B)). The result is quite similar to the literatures although the strain differs from the experiments. This may reflect a common metabolic capability to all *Bdellovibrrios*, since the tested strains in other study and our study has different origin and host dependency.

After 60 min of experiments, the trend of attraction was getting gentle with time. The attraction is only increased by factor 1/4 of attraction from the attraction until 60 minutes. There are several inferences. First, the concentration gradients near the cell inlet cannels become gradual due to the improper washing near the inlet. Second, the IMA cannot quantify too many cells since the cells aggregated and it makes optical interferences. Although, those factors affect some degree of

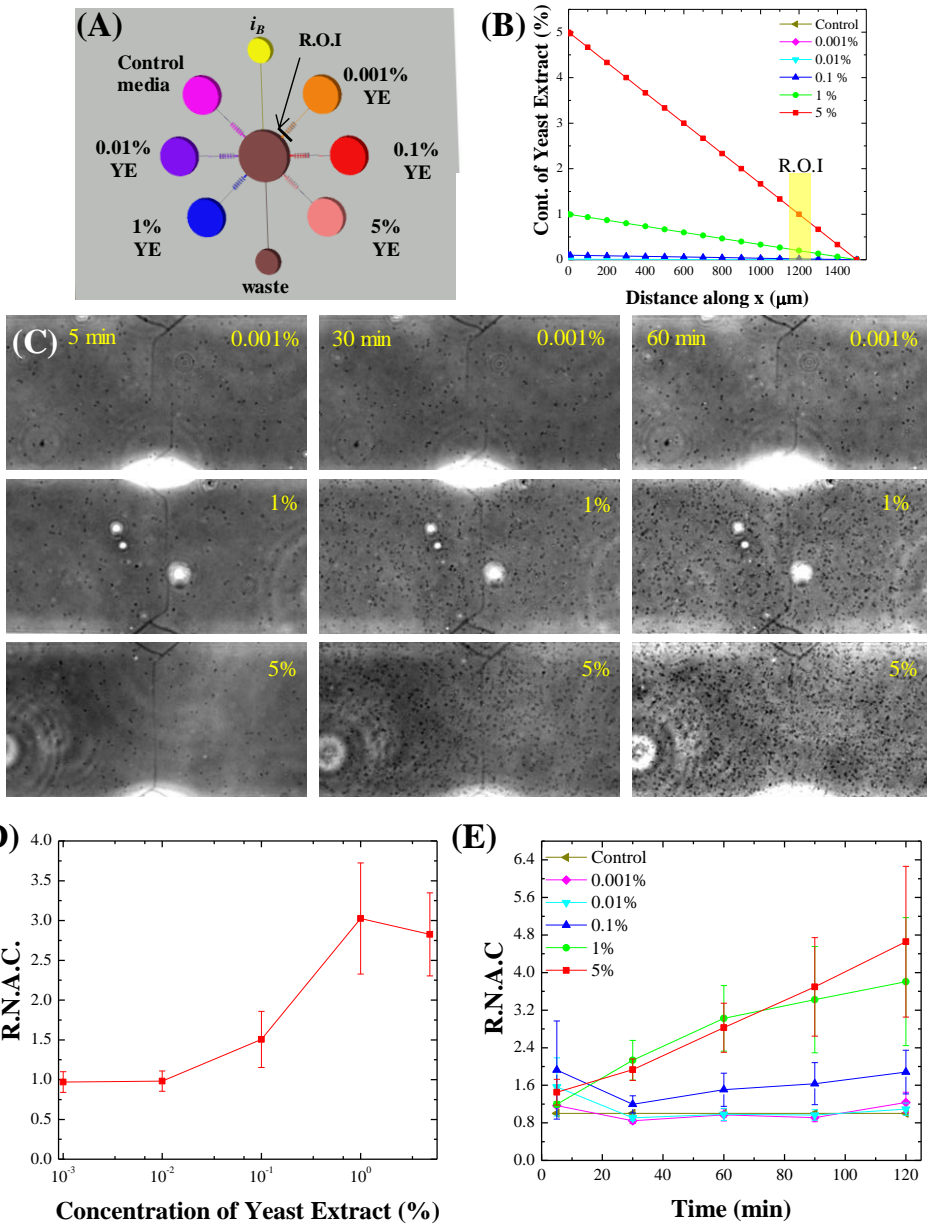


Fig 3.3 Chemotaxis of *B. bacteriovorus* towards various concentrations of yeast extract. (A) Experimental configuration of multi-concentration gradient generator. (B) Theoretical concentration gradient along microchannel at steady state. (C) Attraction of *B. bacteriovorus* towards yeast extract. Black dots indicate single *Bdellovibrio* cells (at 20X magnification). Higher concentration of yeast extract attracts more cells than lower concentration. The area of the region of interest (R.O.I.) is  $160 \times 80 \mu\text{m}^2$  (D) *B. bacteriovorus* shows similar attraction to the control (only DNB) when the concentration of yeast extract is lower than 0.01%. The attraction is linearly increased in higher than 0.01% of yeast extract in log scale. R.N.A.C refers relative number of attracted cells (RNAC = number of attracted cells in the test channel / number of attracted cells in control channel). (E) Quantification of attracted cells with IMA. The number of attracted cells is increased with time. The results show the average of multiple experiments (N=3). The trends become stable within 60minutes.

uncertainties in our experiments and measurements, we quantitatively measure and compare the attractions between compounds in our microfluidic concentration gradient generator.

### 3.2.2 Chemotaxis towards KCl

We also investigated the chemotaxis of *Bdellovibrio* cells (HD 100 strain) towards various concentration of KCl. Since KCl showed strongest attraction for strain UKi2<sup>41</sup>, we tested the compound for strain HD 100. DNB medium samples (40  $\mu$ L) containing 0M (R1), 0.001M (R6), 0.01M (R2), 0.1M (R5), 0.5M (R3), and 1M (R4) of KCl were added to the reservoirs, as shown in Figure 3.4 (A).

Fig. 3.5 (A) shows the accumulation of *B.bacteriovorus* strain HD 100 due to the chemotactic response toward KCl. At 60 minutes, the number of attracted cells was increased as the same pattern as the yeast extract. As shown in the quantification data from Fig.3.4 (A), maximum attraction occurs at initial concentration of 0.1M where the concentration gradient of KCl is 0.03M/ $\mu$ m. The attraction was increased as the concentration of KCl increased, but the attraction was decreased when the concentration of KCl is higher than 0.1M. There are minor attractions occurred at the concentration lower than 0.01M or higher than 0.5M of initial concentration of KCl, compared with control medium. The reasons are the same as the yeast extract case.

The reason of the attraction of *B.bacteriovorus* towards inorganic compounds is not clear but one suggestion is that the inorganic compounds help to maintain the cellular function of bacteria<sup>41</sup>. In addition, it could be help to avoid swimming away from soil particle into open waters where random collision with prey is hardly achieved. Typically, the concentration of potassium in soil solution is about 1 to 5mM and in lake or river water is abou0.36 mM<sup>47</sup> which is close to our result.

As shown in Fig 3.4 (B), the threshold concentration is higher than 0.01M. It is known that threshold concentration of potassium chloride for *B.bacteriovorus* UKi2 strain is about  $10^{-4}$  to  $10^{-5}$ . However, since potassium chloride is not a major attractant for *B.bacteriovorus* HD 100, threshold concentration of KCl for HD 100 strain could be higher than UKi2 strain.

Since the R.N.A.C is just 2 (R.A =  $N_{cells}$ , @ peak concentration /  $N_{cells}$ , @ control medium) at 60 minutes and the R.N.A.C of yeast extract is 3.0, yeast extract is stronger attractant than potassium chloride about 1.5 times for *B.bacteriovorus* strain HD 100.

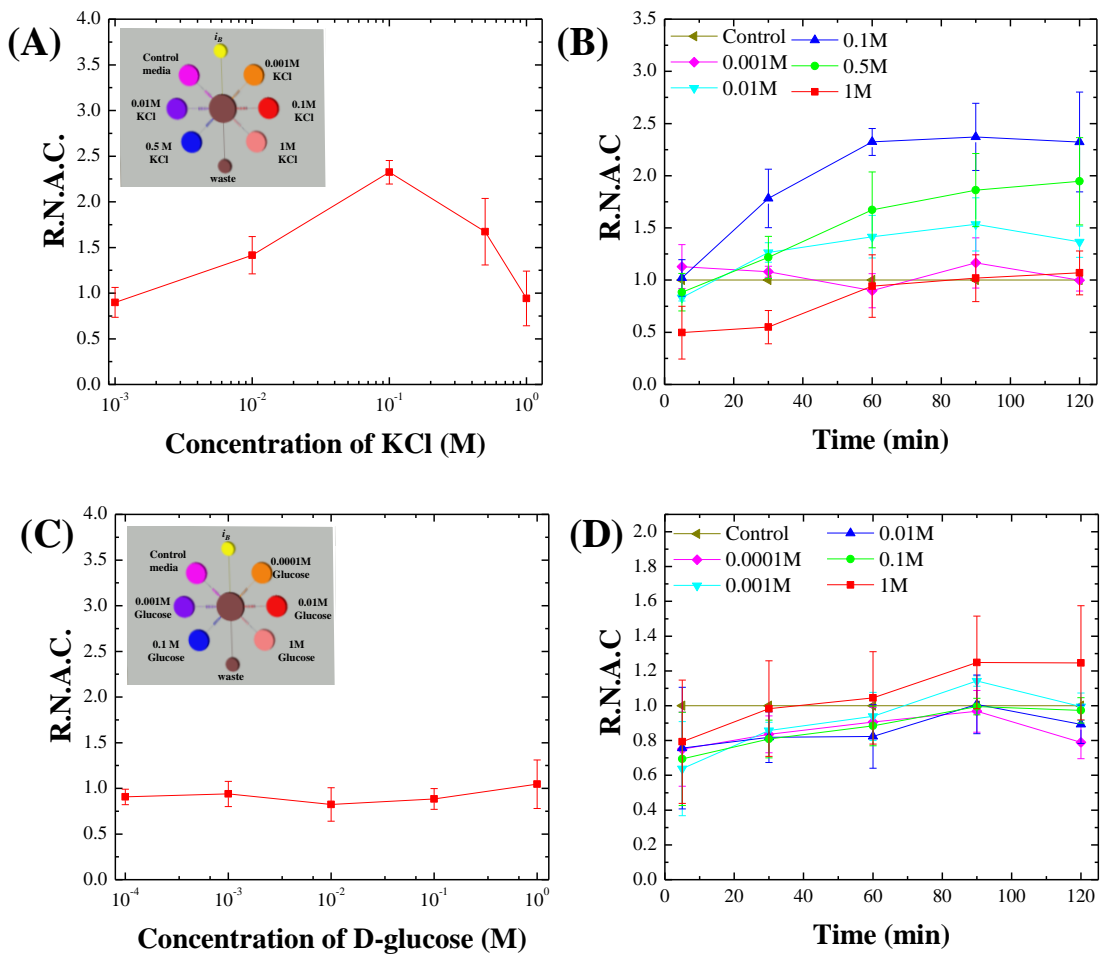


Fig 3.4 Quantitative data for the Chemotaxis assay of *B. bacteriovorus* towards various concentrations of KCl and D-glucose. (A) Quantification of attracted cells along concentration gradient of KCl. The attraction is increased with respect to the concentration of KCl, but the attraction is decreased when the cells exposed to the KCl concentration higher than 0.1M. (B) For KCl gradient, the number of attracted cells is increased with time. The number of attracted cells becomes stable within 60minutes. (C) The attraction of *B. bacteriovorus* towards glucose. *B. bacteriovorus* shows similar attraction to the control (only DNB) regardless to the concentration of D-glucose. (D) For glucose gradient, the number of attracted cells is not change with time.

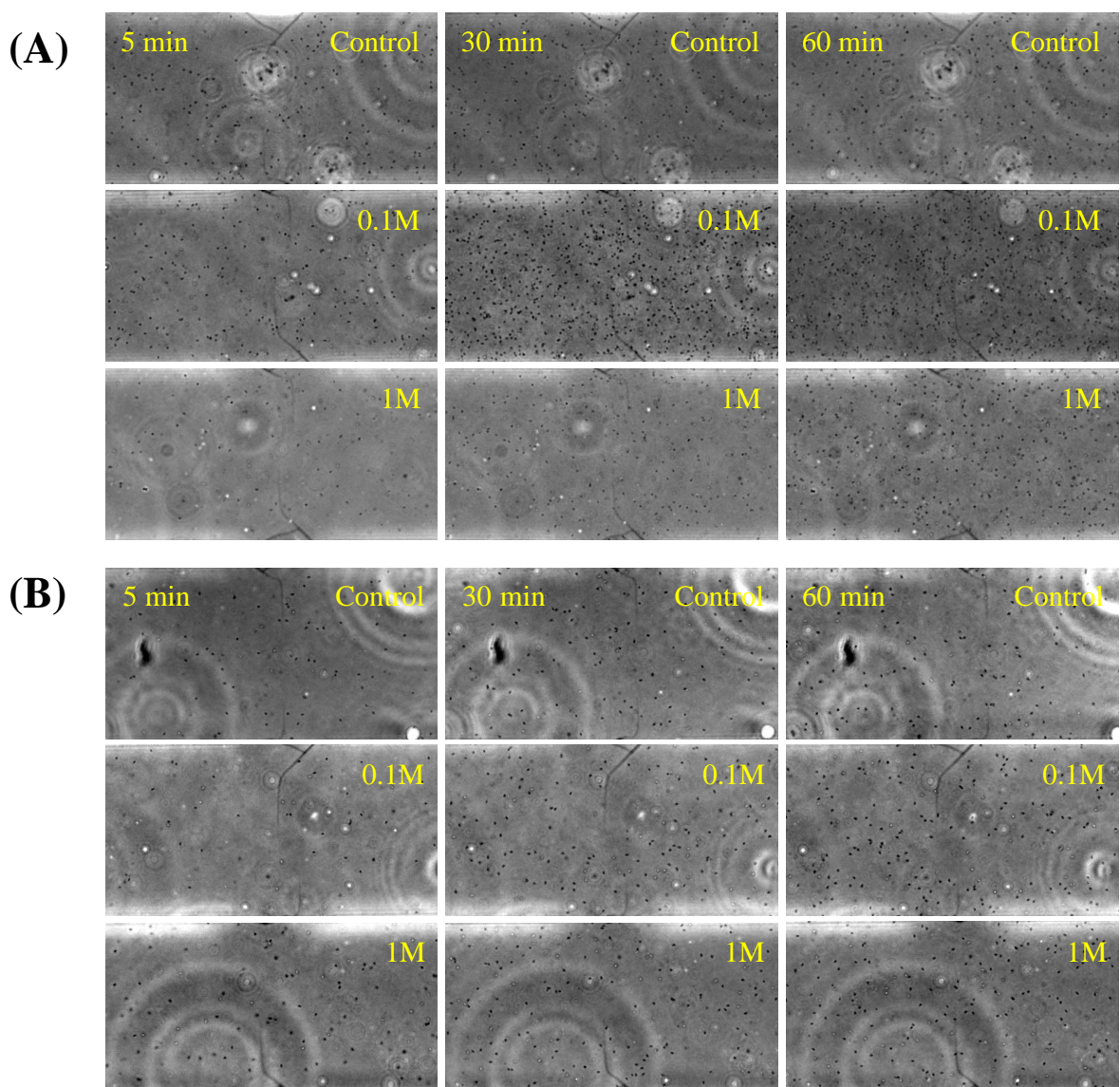


Fig 3.5 Qualitative data for the Chemotaxis assay of *B. bacteriovorus* towards various concentrations of KCl and D-glucose. (A) The attraction of *B. bacteriovorus* towards KCl. The peak concentration is 0.1M. (B) Attraction of *B. bacteriovorus* towards D-glucose. The attraction of *Bdellovibrio* cells was much lower than two other attractants.

### **3.2.3 Chemotaxis towards D-glucose**

It is known that *B.bacteriovorus* strain UKi2 does not shows chemotaxis towards D-glucose. However the same experiment has not been reported for the strain HD 100. The same as our previous experiments, we investigated the chemotaxis of *Bdellovibrio* cells towards various concentration of D-glucose using microfluidic multi-concentration gradient generator. DNB medium samples (40  $\mu\text{L}$ ) containing 0M (R1), 0.0001M (R6), 0.001M (R2), 0.01M (R5), 0.1M (R3), and 1M (R4) of KCl were added to the reservoirs, as shown in Figure 3.4 (C).

Fig. 3.5 (B) shows the accumulation of *B.bacteriovorus* strain HD 100 due to the chemotactic response towards D-glucose. In short, the strain HD 100 does not show any attraction towards D-glucose. The attraction level of all the concentration of glucose was nearly the same as the control medium. It is reasonable because predator cannot metabolite sugar compounds. The only possibility that the predator can show chemotaxis toward sugar is using chemotaxis to locate prey. Therefore, *Bdellovibrio* does not use chemotaxis to locate sources of compounds which could attract and support the growth of prey cells. The results obtained in this experiment are also well consistent with literatures.

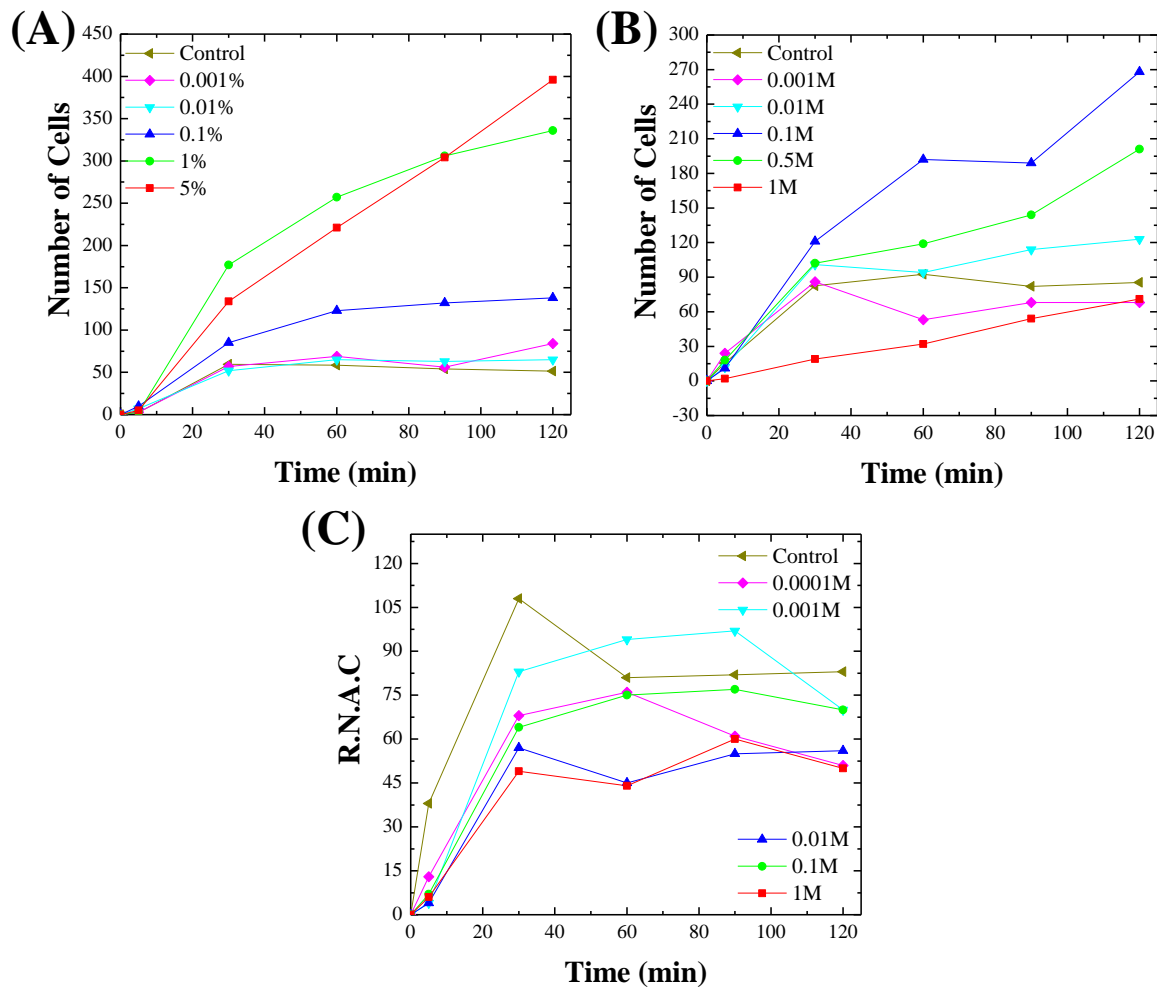


Fig 3.6 Representative figures for each experiment. (A) The number of attracted *B. bacteriovorus* cells towards yeast extract is increased with time. (B) The number of attracted *B. bacteriovorus* cells towards KCl is increased with time. (C) The number of attracted *B. bacteriovorus* cells towards D-glucose is stable with time.

## **Chapter IV**

### **Conclusions**

In this thesis, we investigated response of predatory microbes in various stimuli on our novel microfluidic platform, concentrator array and diffusion based concentration gradient generator.

We developed a concentrator array device that can concentrate prey and predator cells in a mechanically confined chamber by utilizing both the motility of bacteria and the microfabricated arrowhead-shaped ratchet structures. Since the device was integrated with two types of microfluidic cell mixing channel networks that are similar to the Christmas tree-shaped concentration gradient generator, 9 different experimental configurations were possible on a single chip. Using the device, we demonstrated that the use of microfluidic concentrator arrays was useful in studying the predation rates of *B. bacteriovorus* toward bacterial strains (*E. coli*) at both a single and multiple cell level. In addition, we demonstrated that the device compartmentalizes predator cells so that it was possible to conduct control and predation experiment simultaneously. Furthermore, we demonstrated that the device generates linear concentration gradients of prey and/or predatory cells so that the effect of the ratios of prey to predator densities on the predation behaviour/rates can be quantified at a time. All these different experiments can be performed on a chip made of a single microfluidic channel network which allows us to study many different conditions with a single set of cultures.

We also investigated chemotaxis of *B.bacteriovorus* towards three different attractants with various concentration gradients on our microfluidic multi concentration gradient generator. Attractions towards yeast extract and potassium chloride are about 3 and 2 times stronger than control attraction at the peak concentration, in the presence of concentration gradient. The strongest attractant for *B.bacteriovorus* HD 100 strain within the tested compounds was yeast extract. There is no attraction toward sugar source such as D-glucose therefore *B.bacteriovorus* does not use chemotaxis toward sugar source to locate their potential prey. These results are well consistence with literatures.

Since these novel microfluidic devices can provide accurate gradient and defined geometry, we believe that, they are not only useful means for the study of microbial predations and chemotaxis but it also would be broadly used in other microbial biotechnological applications.

## REFERENCES

- [1] Markelova, N. Y. 2007, 'Survival strategy of Bdellovibrio', *Microbiology*, vol. 76, no. 6, pp. 769-74.
- [2] Sockett, R. E. 2009, 'Predatory Lifestyle of Bdellovibrio bacteriovorus', *Annual Review of Microbiology*, vol. 63, pp. 523-39.
- [3] Chauhan, A., Fortenberry, G. Z., Lewis, D. E. & Williams, H. N. 2009, 'Increased Diversity of Predacious Bdellovibrio-Like Organisms (BLOs) as a Function of Eutrophication in Kumaon Lakes of India', *Current Microbiology*, vol. 59, no. 1, pp. 1-8.
- [4] Yair, S., Yaacov, D., Susan, K. & Jurkewitch, E. 2003, 'Small eats big: ecology and diversity of Bdellovibrio and like organisms, and their dynamics in predator-prey interactions', *Agronomie*, vol. 23, no. 5-6, pp. 433-9.
- [5] Sockett, R. E. & Lambert, C. 2004, 'Bdellovibrio as therapeutic agents: a predatory renaissance?', *Nature Reviews Microbiology*, vol. 2, no. 8, pp. 669-75.
- [6] El-Ali, J., Sorger, P. K. & Jensen, K. F. 2006, 'Cells on chips', *Nature*, vol. 442, no. 7101, pp. 403-11.
- [7] Liu, W. T. & Zhu, L. 2005, 'Environmental microbiology-on-a-chip and its future impacts', *Trends in Biotechnology*, vol. 23, no. 4, pp. 174-9.
- [8] Abhyankar, V. V. & Beebe, D. J. 2007, 'Spatiotemporal micropatterning of cells on arbitrary substrates', *Analytical Chemistry*, vol. 79, no. 11, pp. 4066-73.
- [9] Weibel, D. B., DiLuzio, W. R. & Whitesides, G. M. 2007, 'Microfabrication meets microbiology', *Nature Reviews Microbiology*, vol. 5, no. 3, pp. 209-18.
- [10] Englert, D. L., Manson, M. D. & Jayaraman, A. 2010, 'Investigation of bacterial chemotaxis in flow-based microfluidic devices', *Nature Protocols*, vol. 5, no. 5, pp. 864-72.
- [11] Jeon, N. L., Baskaran, H., Dertinger, S. K. W., Whitesides, G. M., Van de Water, L. & Toner, M. 2002, 'Neutrophil chemotaxis in linear and complex gradients of interleukin-8 formed in a microfabricated device', *Nature Biotechnology*, vol. 20, no. 8, pp. 826-30.
- [12] Kim, M. & Kim, T. 2010, 'Diffusion-Based and Long-Range Concentration Gradients of Multiple Chemicals for Bacterial Chemotaxis Assays', *Analytical Chemistry*, vol. 82, no. 22, pp. 9401-9.
- [13] Biondi, S. A., Quinn, J. A. & Goldfine, H. 1998, 'Random motility of swimming bacteria in restricted geometries', *Aiche Journal*, vol. 44, no. 8, pp. 1923-9.
- [14] Kim, S. Y., Lee, E. S., Lee, H. J., Lee, S. Y., Lee, S. K. & Kim, T. 2010, 'Microfabricated ratchet structures for concentrating and patterning motile bacterial cells', *Journal of Micromechanics and Microengineering*, vol. 20, no. 9, pp. -.
- [15] DiLuzio, W. R., Turner, L., Mayer, M., Garstecki, P., Weibel, D. B., Berg, H. C. & Whitesides, G. M. 2005, 'Escherichia coli swim on the right-hand side', *Nature*, vol. 435, no. 7046, pp. 1271-4.

- [16] Galajda, P., Keymer, J., Dalland, J., Park, S., Kou, S. & Austin, R. 2008, 'Funnel ratchets in biology at low Reynolds number: choanotaxis', *Journal of Modern Optics*, vol. 55, no. 19-20, pp. 3413-22.
- [17] Hulme, S. E., DiLuzio, W. R., Shevkoplyas, S. S., Turner, L., Mayer, M., Berg, H. C. & Whitesides, G. M. 2008, 'Using ratchets and sorters to fractionate motile cells of Escherichia coli by length', *Lab on a Chip*, vol. 8, no. 11, pp. 1888-95.
- [18] Galajda, P., Keymer, J., Chaikin, P. & Austin, R. 2007, 'A wall of funnels concentrates swimming bacteria', *Journal of Bacteriology*, vol. 189, no. 23, pp. 8704-7.
- [19] Hiratsuka, Y., Tada, T., Oiwa, K., Kanayama, T. & Uyeda, T. Q. P. 2001, 'Controlling the direction of kinesin-driven microtubule movements along microlithographic tracks', *Biophysical Journal*, vol. 81, no. 3, pp. 1555-61.
- [20] Kim, T., Cheng, L. J., Kao, M. T., Hasselbrink, E. F., Guo, L. J. & Meyhofer, E. 2009, 'Biomolecular motor-driven molecular sorter', *Lab on a Chip*, vol. 9, no. 9, pp. 1282-5.
- [21] Ahmed, T., Shimizu, T. S. & Stocker, R. 2010, 'Bacterial Chemotaxis in Linear and Nonlinear Steady Microfluidic Gradients', *Nano Letters*, vol. 10, no. 9, pp. 3379-85.
- [22] Englert, D. L., Manson, M. D. & Jayaraman, A. 2009, 'Flow-Based Microfluidic Device for Quantifying Bacterial Chemotaxis in Stable, Competing Gradients', *Applied and Environmental Microbiology*, vol. 75, no. 13, pp. 4557-64.
- [23] Kalinin, Y., Neumann, S., Sourjik, V. & Wu, M. M. 2010, 'Responses of Escherichia coli Bacteria to Two Opposing Chemoattractant Gradients Depend on the Chemoreceptor Ratio', *Journal of Bacteriology*, vol. 192, no. 7, pp. 1796-800.
- [24] Watanabe, K., Nakagawa, H. & Tsurufuji, S. 1985, 'A New Simple Plastic Chemotaxis Device of the Boyden Chamber Type Utilizing an Immunoassay Plate', *Japanese Journal of Pharmacology*, vol. 39, no. 1, pp. 102-4.
- [25] Sawano, K., Sakano, T., Kagoishi, Y., Yoshimitsu, H., Miyake, Y., Kobayashi, Y. & Usui, T. 1979, 'Chemotaxis of Granulocytes in Chediak-Higashi-Syndrome with Agarose Plate and Filter Chamber Methods', *Hiroshima Journal of Medical Sciences*, vol. 28, no. 2, pp. 107-13.
- [26] Bainer, R., Park, H. & Cluzel, P. 2003, 'A high-throughput capillary assay for bacterial chemotaxis', *Journal of Microbiological Methods*, vol. 55, no. 1, pp. 315-9.
- [27] Whitesides, G. M. 2006, 'The origins and the future of microfluidics', *Nature*, vol. 442, no. 7101, pp. 368-73.
- [28] Cheng, S. Y., Heilman, S., Wasserman, M., Archer, S., Shuler, M. L. & Wu, M. M. 2007, 'A hydrogel-based microfluidic device for the studies of directed cell migration', *Lab on a Chip*, vol. 7, no. 6, pp. 763-9.
- [29] Varon, M. & Shilo, M. 1968, 'Interaction of Bdellovibrio Bacteriovorus and Host Bacteria .I. Kinetic Studies of Attachment and Invasion of Escherichia Coli B by Bdellovibrio Bacteriovorus', *Journal of Bacteriology*, vol. 95, no. 3, pp. 744-&.

- [30] Varon, M. & Shilo, M. 1969, 'Interaction of Bdellovibrio Bacteriovorus and Host Bacteria .2. Intracellular Growth and Development of Bdellovibrio Bacteriovorus in Liquid Cultures', *Journal of Bacteriology*, vol. 99, no. 1, pp. 136-&.
- [31] Seidler, R. J. & Starr, M. P. 1969, 'Factors affecting the intracellular parasitic growth of Bdellovibrio bacteriovorus developing within Escherichia coli', *Journal of Bacteriology*, vol. 97, no. 2, pp. 912-23.
- [32] Kim, T., Pinelis, M. & Maharbiz, M. M. 2009, 'Generating Steep Shear-free Gradients of Small Molecules for Cell Culture', *Biomedical Microdevices*, vol. 11, no. 1, pp. 65-73.
- [33] Starr, M. P. & Baigent, N. L. 1966, 'Parasitic interaction of Bdellovibrio bacteriovorus with other bacteria', *Journal of Bacteriology*, vol. 91, no. 5, pp. 2006-17.
- [34] Barel, G., Sirota, A., Volpin, H. & Jurkewitch, E. 2005, 'Fate of predator and prey proteins during growth of Bdellovibrio bacteriovorus on Escherichia coli and Pseudomonas syringae prey', *Journal of Bacteriology*, vol. 187, no. 1, pp. 329-35.
- [35] Sanchez-Amat, A. & Torrella, F. 1990, 'Formation of stable bdelloplasts as a starvation-survival strategy of marine bdellovibrios', *Appl Environ Microbiol*, vol. 56, no. 9, pp. 2717-25.
- [36] Slade, K. M., Baker, R., Chua, M., Thompson, N. L. & Pielak, G. J. 2009, 'Effects of recombinant protein expression on green fluorescent protein diffusion in Escherichia coli', *Biochemistry*, vol. 48, no. 23, pp. 5083-9.
- [37] Binz, M., Lee, A. P., Edwards, C. & Nicolau, D. V. 2010, 'Motility of bacteria in microfluidic structures', *Microelectronic Engineering*, vol. 87, no. 5-8, pp. 810-3.
- [38] Lamarre, A. G., Straley, S. C. & Conti, S. F. 1977, 'Chemotaxis toward Amino-Acids by Bdellovibrio-Bacteriovorus', *Journal of Bacteriology*, vol. 131, no. 1, pp. 201-7.
- [39] Straley, S. C. & Conti, S. F. 1974, 'Chemotaxis in Bdellovibrio-Bacteriovorus', *Journal of Bacteriology*, vol. 120, no. 1, pp. 549-51.
- [40] Straley, S. C. & Conti, S. F. 1977, 'Chemotaxis by Bdellovibrio-Bacteriovorus toward Prey', *Journal of Bacteriology*, vol. 132, no. 2, pp. 628-40.
- [41] Straley, S. C., Lamarre, A. G., Lawrence, L. J. & Conti, S. F. 1979, 'Chemotaxis of Bdellovibrio-Bacteriovorus toward Pure Compounds', *Journal of Bacteriology*, vol. 140, no. 2, pp. 634-42.
- [42] Adler, J. 1969, 'Chemoreceptors in Bacteria', *Science*, vol. 166, no. 3913, pp. 1588-&.
- [43] Rendulic, S., Jagtap, P., Rosinus, A., Eppinger, M., Baar, C., Lanz, C., Keller, H., Lambert, C., Evans, K. J., Goesmann, A., Meyer, F., Sockett, R. E. & Schuster, S. C. 2004, 'A predator unmasked: Life cycle of Bdellovibrio bacteriovorus from a genomic perspective', *Science*, vol. 303, no. 5658, pp. 689-92.
- [44] Lambert, C., Smith, M. C. M. & Sockett, R. E. 2003, 'A novel assay to monitor predator-prey interactions for Bdellovibrio bacteriovorus 109 J reveals a role for methyl-accepting chemotaxis proteins in predation', *Environmental Microbiology*, vol. 5, no. 2, pp. 127-32.
- [45] Rogosky, A. M., Moak, P. L. & Emmert, E. A. B. 2006, 'Differential predation by Bdellovibrio bacteriovorus 109J', *Current Microbiology*, vol. 52, no. 2, pp. 81-5.

[46] Adler, J., Hazelbau.Gl & Dahl, M. M. 1973, 'Chemotaxis toward Sugars in Escherichia-Coli', *Journal of Bacteriology*, vol. 115, no. 3, pp. 824-47.

[47] Mishusti.Ne 1972, 'Estimation of Construction of a System of Plant Mineral Nutrition', *Izvestiya Akademii Nauk Sssr Seriya Biologicheskaya*, no. 1, pp. 88-&.